Published for SISSA by Springer

Received: *July 3, 2014*
Revised: *July 30, 2014*
Accepted: *August 4, 2014*
Published: *August 25, 2014*

A to Z of Flavour with Pati-Salam

Stephen F. King

School of Physics and Astronomy, University of Southampton, Southampton, SO17 1BJ, United Kingdom

E-mail: king@soton.ac.uk

Abstract: We propose an elegant theory of flavour based on $A_4 \times Z_5$ family symmetry with Pati-Salam unification which provides an excellent description of quark and lepton masses, mixing and CP violation. The A_4 symmetry unifies the left-handed families and its vacuum alignment determines the columns of Yukawa matrices. The Z_5 symmetry distinguishes the right-handed families and its breaking controls CP violation in both the quark and lepton sectors. The Pati-Salam symmetry relates the quark and lepton Yukawa matrices, with $Y^u = Y^\nu$ and $Y^d \sim Y^e$. Using the see-saw mechanism with very hierarchical right-handed neutrinos and CSD4 vacuum alignment, the model predicts the entire PMNS mixing matrix and gives a Cabibbo angle $\theta_C \approx 1/4$. In particular, for a discrete choice of Z_5 phases, it predicts maximal atmospheric mixing, $\theta_{23}^l = 45^\circ \pm 0.5^\circ$ and leptonic CP violating phase $\delta^l = 260^\circ \pm 5^\circ$. The reactor angle prediction is $\theta_{13}^l = 9^\circ \pm 0.5^\circ$, while the solar angle is $34^\circ \gtrsim \theta_{12}^l \gtrsim 31^\circ$, for a lightest neutrino mass in the range $0 \lesssim m_1 \lesssim 0.5$ meV, corresponding to a normal neutrino mass hierarchy and a very small rate for neutrinoless double beta decay.

Keywords: Neutrino Physics, Discrete and Finite Symmetries

ArXiv ePrint: 1406.7005

doi:10.1007/JHEP08(2014)130

JHEP08(2014)130

Contents

JHEP08(2014)130

1 Introduction

The problem of understanding the quark and lepton masses, mixing angles and CP violating phases remains one of the most fascinating puzzles in particle physics. Following the discovery of a Standard Model (SM)-like Higgs boson at the LHC [1, 2], it seems highly plausible that quark masses, mixing angles and CP phase originate from Yukawa couplings to a Higgs field. However the SM offers absolutely no insight into the origin or nature of these Yukawa couplings, motivating approaches beyond the SM [3, 4].

In the quark sector, the Yukawa couplings are organised into 3×3 quark Yukawa matrices Y^u and Y^d, which must be responsible for the quark mass hierarchies and small quark mixing angles, together with the CP phase. Similarly, the charged lepton Yukawa matrix Y^e must lead to a mass hierarchy similar to that of the down-type quarks. The origin of small quark mixing and CP violation and the strong mass hierarchies of the quarks and charged leptons, with an especially strong hierarchy in the up-type quark sector, is simply unexplained within the SM. The nine charged fermion masses, three quark mixing angles, including the largest Cabibbo angle $\theta_C \approx 13^\circ$, and the CP phase are all determined from experiment. From a more fundamental point of view, the three Yukawa matrices Y^u, Y^d and Y^e contain 54 undetermined Yukawa couplings leading to 13 physical observables with a calculable scale dependence [5, 6].

Following the discovery of atmospheric neutrino oscillations by Super-Kamiokande in 1998 and solar neutrino oscillations by SNO in 2002 [7, 8], Daya Bay has recently accurately measured a non-zero reactor angle [9] which rules out tri-bimaximal (TB) [10] mixing. However, recent global fits [11–13][1] are consistent with tri-bimaximal-Cabibbo (TBC) [14] mixing, based on the TB atmospheric angle $\theta_{23}^l \approx 45^\circ$, the TB solar angle $\theta_{12}^l \approx 35^\circ$ and a reactor angle $\theta_{13}^l \approx \theta_C/\sqrt{2} \approx 9^\circ$. The extra parameters of the lepton sector include three neutrino masses, three lepton mixing angles and up to three CP phases, although no leptonic CP violation has yet been observed and the lightest neutrino mass has not been measured. The 9 additional neutrino observables, together with the 13 physical observables in the charged fermion sector, requires 22 unexplained parameters in the flavour sector of the SM. This provides a powerful motivation to search for theories of flavour (TOF) based on discrete family symmetry which contain fewer parameters [15, 16].

The origin of neutrino mass is presently unknown and certainly requires some extension of the SM, even if only by the addition of right-handed (RH) neutrinos which are singlets under the SM gauge group. Since such RH neutrinos may have large Majorana masses, in excess of the electroweak breaking scale, such a minimal extension naturally leads to the idea of a see-saw mechanism [17–20], resulting from a neutrino Yukawa matrix Y^ν, together with a complex symmetric Majorana matrix M_R of heavy right-handed neutrinos, leading to a light effective Majorana neutrino mass matrix $m^\nu \sim v^2 Y^\nu M_R^{-1} Y^{\nu T}$, where v is the Higgs vacuum expectation value (VEV). However the see-saw mechanism does not explain large lepton mixing angles, with the smallest being the reactor angle $\theta_{13}^l \approx 9^\circ$, nor does it address any of the flavour puzzles in the charged fermion sector.

[1] An updated version of the results in [13] can be found at the website www.nu-fit.org, see the link therein: "v1.2: Three- neutrino results after the TAUP 2013 Conference".

JHEP08(2014)130

The origin of large lepton mixing may be accounted for within the see-saw mechanism with the aid of sequential dominance (SD) [21–23]. For example, with an approximately diagonal M_R, the lightest right-handed neutrino $\nu_R^{\rm atm}$ may give the dominant contribution to the atmospheric neutrino mass m_3, the second lightest right-handed neutrino $\nu_R^{\rm sol}$ to the solar neutrino mass m_2 and the heaviest, almost decoupled, right-handed neutrino $\nu_R^{\rm dec}$ may be responsible for the lightest neutrino mass m_1. The immediate prediction of SD is a normal neutrino mass hierarchy, $m_3 > m_2 \gg m_1$, which will be tested in the near future. However SD also provides a simple way to account for maximal atmospheric mixing and tri-maximal solar mixing by adding constraints to the first two columns of the neutrino Yukawa matrix Y^ν, with the third column assumed to be approximately decoupled from the see-saw mechanism. In the diagonal Y^e basis, if the dominant first column of Y^ν is proportional to $(0,1,1)^T$ then this implies a maximal atmospheric angle $\tan\theta_{23}^l \approx 1$ [24]. This could be achieved with a non-Abelian family symmetry such as A_4 [25], if the first column is generated by a triplet flavon field with a vacuum alignment proportional to $(0,1,1)^T$. In such models, it has been shown that the vacuum alignment completely breaks the A_4 symmetry, and such models are therefore referred to as "indirect" models [26]. Such "indirect" models are highly predictive and do not require such large discrete groups as the "direct" models where the Klein symmetry of the neutrino mass matrix is identified as a subgroup of the family symmetry [27–29].

Constrained sequential dominance (CSD) [30] involves the dominant right-handed neutrino $\nu_R^{\rm atm}$ mainly responsible for the atmospheric neutrino mass having couplings to $(\nu_e, \nu_\mu, \nu_\tau)$ proportional to $(0,1,1)$, as above, while the subdominant right-handed neutrino $\nu_R^{\rm sol}$ giving the solar neutrino mass has various couplings to $(\nu_e, \nu_\mu, \nu_\tau)$ as follows:

- CSD1: $(1,1,-1)$ leading to TB mixing with zero reactor angle $\theta_{13}^l \approx 0^\circ$ [30].
- CSD2: $(1,2,0)$ giving $\theta_{13}^l \approx 6^\circ$ [31, 32].
- CSD3: $(1,3,1)$ with a relative phase $\pm\pi/3$ giving $\theta_{13}^l \approx 8.5^\circ$ [33].
- CSD4: $(1,4,2)$, with a relative phase $\pm 2\pi/5$ giving $\theta_{13}^l \approx 9^\circ$ [33, 34].

"Indirect" models of leptons have been constructed based on A_4 using both CSD3 [33] and CSD4 [34] since these are the most promising from the point of view of the reactor angle. From the point of view of extending to the quark sector, CSD4 seems to be the most promising since in unified models with $Y^u = Y^\nu$, the second column is proportional to $(1,4,2)^T$. This simultaneously provides a prediction for both lepton mixing and the Cabibbo angle $\theta_C \approx 1/4$ in the diagonal $Y^d \sim Y^e$ basis [35].

The model in [35] was based on A_4 family symmetry with $Z_3^4 \times Z_5^5$ and quark-lepton unification via the Pati-Salam (PS) [36] gauge subgroup $\mathrm{SU}(4)_{PS} \times \mathrm{SU}(2)_L \times \mathrm{U}(1)_R$ and the CSD4 alignment $(1,4,2)$. The small quark mixing angles arose from higher order (HO) corrections appearing in Y^u and Y^ν, providing a theoretical error or noise which blurred the PMNS predictions. Here we discuss an alternative A_4 model which has three advantages over the previous model. Firstly it is more unified, being based on the full PS gauge group $\mathrm{SU}(4)_{PS} \times \mathrm{SU}(2)_L \times \mathrm{SU}(2)_R$ [36]. Secondly it introduces only a single Z_5 symmetry,

JHEP08(2014)130

replacing the rather cumbersome $Z_3^4 \times Z_5^5$ symmetry. Thirdly, it accounts for small quark mixing angles already at the leading order (LO), with all Higher Order (HO) corrections being rather small, leading to more precise predictions for the PMNS parameters, such as maximal atmospheric mixing. Unlike other $A_4 \times$PS models (see e.g. [37]), the present model does not involve any Abelian U(1) family symmetry. Instead the left-handed PS fermions are unified into a triplet of A_4 while the right-handed PS fermions are distinguished by Z_5, as in figure 1.

In the present paper, then, we propose a rather elegant TOF based on the PS gauge group combined with a discrete $A_4 \times Z_5$ family symmetry. PS unification relates quark and lepton Yukawa matrices and in particular predicts equal up-type quark and neutrino Yukawa matrices $Y^u = Y^\nu$, leading to Dirac neutrino masses being equal to up, charm and top masses. The see-saw mechanism then implies very hierarchical right-handed neutrinos. The A_4 family symmetry determines the structure of Yukawa matrices via the CSD4 vacuum alignment [33, 34], with the three columns of $Y^u = Y^\nu$ being proportional to $(0, 1, 1)^T$, $(1, 4, 2)^T$ and $(0, 0, 1)^T$, respectively, where each column has an overall phase determined by Z_5 breaking, which controls CP violation in both the quark and lepton sectors. The down-type quark and charged lepton Yukawa matrices are both approximately equal and diagonal $Y^d \sim Y^e$, but contain small off-diagonal elements responsible for the small quark mixing angles θ_{13}^q and θ_{23}^q. The model predicts the Cabibbo angle $\theta_C \approx 1/4$, up to such small angle corrections. The main limitation of the model is that it describes the fermion masses and small quark mixing angles by 16 free parameters. The main success of the model is that, since there are 6 fewer parameters than the 22 flavour observables, it predicts the entire PMNS lepton mixing matrix including the three lepton mixing angles and the three leptonic CP phases. The model may be tested quite soon via its prediction of maximal atmospheric mixing with a normal neutrino mass hierarchy.

The layout of the remainder of the paper is as follows. In section 2, we give a brief overview of the essential features of the model. In section 3, we present the full model and show how the messenger sector can lead to effective operators, then discuss how these operators lead to Yukawa and Majorana mass matrices. In section 4, we derive the quark masses and mixing, including CP violation, arising from the quark Yukawa matrices, first analytically, then numerically. In section 5, we implement the see-saw mechanism, then consider the resulting neutrino masses and lepton mixing, with modified Georgi-Jarlskog relations, before performing a full numerical analysis of neutrino masses and lepton mixing, including CP violation. In section 6, we consider higher order corrections to the results and show that they are small due to the particular messenger sector. Finally section 7 concludes the paper. A_4 group theory is discussed in appendix A and the origin of the light Higgs doublets H_u and H_d in appendix B.

2 Overview of the model

2.1 Symmetries of the model

The model is based on the Pati-Salam gauge group [36], with $A_4 \times Z_5$ family symmetry,

$$\mathrm{SU}(4)_C \times \mathrm{SU}(2)_L \times \mathrm{SU}(2)_R \times A_4 \times Z_5. \tag{2.1}$$

JHEP08(2014)130

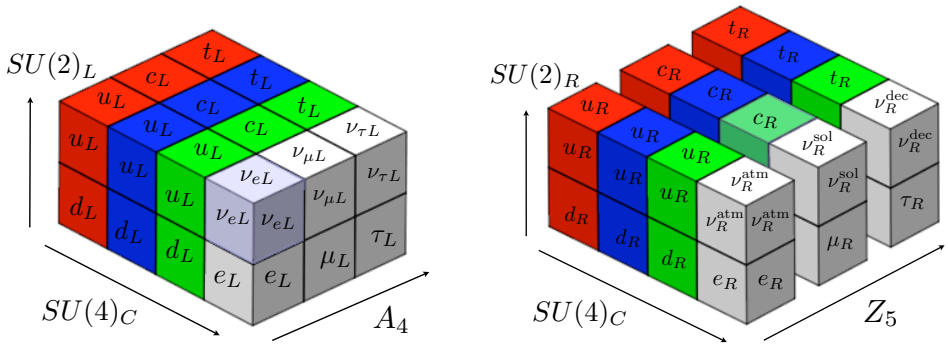

Figure 1. A to Z of flavour with Pati-Salam, where $A \equiv A_4$ and $Z \equiv Z_5$. The left-handed families form a triplet of A_4 and are doublets of $\mathrm{SU}(2)_L$. The right-handed families are distinguished by Z_5 and are doublets of $\mathrm{SU}(2)_R$. The $\mathrm{SU}(4)_C$ unifies the quarks and leptons with leptons as the fourth colour, depicted here as white.

The quarks and leptons are unified in the PS representations as follows,

$$F_i = (4,2,1)_i = \begin{pmatrix} u & u & u & \nu \\ d & d & d & e \end{pmatrix}_i \to (Q_i, L_i),$$
$$F_i^c = (\bar{4},1,2)_i = \begin{pmatrix} u^c & u^c & u^c & \nu^c \\ d^c & d^c & d^c & e^c \end{pmatrix}_i \to (u_i^c, d_i^c, \nu_i^c, e_i^c), \tag{2.2}$$

where the SM multiplets $Q_i, L_i, u_i^c, d_i^c, \nu_i^c, e_i^c$ resulting from PS breaking are also shown and the subscript i $(= 1,2,3)$ denotes the family index. The left-handed quarks and leptons form an A_4 triplet F, while the three (CP conjugated) right-handed fields F_i^c are A_4 singlets, distinguished by Z_5 charges $\alpha, \alpha^3, 1$, for $i = 1,2,3$, respectively. Clearly the Pati-Salam model cannot be embedded into an SO(10) Grand Unified Theory (GUT) since different components of the 16-dimensional representation of SO(10) would have to transform differently under $A_4 \times Z_5$, which is impossible. On the other hand, the PS gauge group and A_4 could emerge directly from string theory (see e.g. [38–40]).

2.2 Pati-Salam breaking

The Pati-Salam gauge group is broken at the GUT scale to the SM,

$$\mathrm{SU}(4)_C \times \mathrm{SU}(2)_L \times \mathrm{SU}(2)_R \to \mathrm{SU}(3)_C \times \mathrm{SU}(2)_L \times \mathrm{U}(1)_Y, \tag{2.3}$$

by PS Higgs, H^c and $\overline{H^c}$,

$$H^c = (\bar{4},1,2) = (u_H^c, d_H^c, \nu_H^c, e_H^c),$$
$$\overline{H^c} = (4,1,2) = (\bar{u}_H^c, \bar{d}_H^c, \bar{\nu}_H^c, \bar{e}_H^c). \tag{2.4}$$

These acquire vacuum expectation values (VEVs) in the "right-handed neutrino" directions, with equal VEVs close to the GUT scale 2×10^{16} GeV,

$$\langle H^c \rangle = \langle \nu_H^c \rangle = \langle \overline{H^c} \rangle = \langle \bar{\nu}_H^c \rangle \sim 2 \times 10^{16} \text{ GeV}, \tag{2.5}$$

JHEP08(2014)130

so as to maintain supersymmetric gauge coupling unification. Since the PS Higgs fields do not carry any $A_4 \times Z_5$ charges, the potential responsible for supersymmetric PS breaking considered in [41] is assumed to be responsible for PS breaking here.

2.3 CP violation

Our starting point is to assume that the high energy theory, above the PS breaking scale, conserves CP [42, 43]. We shall further assume that CP is spontaneously broken by the complex VEVs of scalar fields which spontaneously break A_4 and Z_5. The scalars include A_4 triplets $\phi \sim 3$, A_4 singlets $\xi \sim 1$, and other one dimensional A_4 representations such as $\Sigma_u \sim 1'$ and $\Sigma_d \sim 1''$. In addition all of the above fields carry Z_5 charges denoted as the powers α^n, where $\alpha = e^{2\pi i/5}$ and n is an integer. For example $\xi \sim \alpha^4$ under Z_5. The group theory of A_4 is reviewed in appendix A, while Z_5 corresponds to $\alpha^5 = 1$.

Under a CP transformation, the A_4 singlet fields transform into their complex conjugates [44, 45],

$$\xi \to \xi^*, \qquad \Sigma_u \to \Sigma_u^*, \qquad \Sigma_d \to \Sigma_d^*, \tag{2.6}$$

where the complex conjugate fields transform in the complex conjugate representations under $A_4 \times Z_5$. For example if $\xi \sim \alpha^4$, under Z_5, then $\xi^* \sim \alpha$. Similarly if $\Sigma_u \sim 1'$, $\Sigma_d \sim 1''$, under A_4, then $\Sigma_u^* \sim 1''$, $\Sigma_d^* \sim 1'$. On the other hand, in the Ma-Rajarsakaran [25] basis of appendix A, for A_4 triplets $\phi \sim (\phi_1, \phi_2, \phi_3)$, a consistent definition of CP symmetry requires the second and third triplet components to swap under CP [44, 45],

$$\phi \to (\phi_1^*, \phi_3^*, \phi_2^*). \tag{2.7}$$

CP violation has also been considered in a variety of other discrete groups [46–51]. With the above definition of CP, all coupling constants g and explicit masses m are real due to CP conservation and the only source of phases can be the VEVs of fields which break $A_4 \times Z_5$. In the model of interest, all the physically interesting CP phases will arise from Z_5 breaking as in [42, 43].

For example, consider the A_4 singlet field ξ which carries a Z_5 charge α^4. The VEV of this field arises from Z_5 invariant quintic terms in the superpotential [42, 43],

$$gP\left(\frac{\xi^5}{\Lambda^3} - m^2\right) \tag{2.8}$$

where, as in [42, 43], P denotes a singlet and the coupling g and mass m are real due to CP conservation. The F-term condition from eq. (2.8) is,

$$\left|\frac{\langle\xi\rangle^5}{\Lambda^3} - m^2\right|^2 = 0. \tag{2.9}$$

This is satisfied, for example, by $\langle\xi\rangle = |(\Lambda^3 m^2)^{1/5}| e^{-4i\pi/5}$, where we arbitrarily select the phase to be $-4\pi/5$ from amongst a discrete set of five possible choices, which are not distinguished by the F-term condition, as in [34]. We emphasise that CP breaking is controlled by the Abelian Z_5 symmetry rather than the non-Abelian A_4 symmetry.

JHEP08(2014)130

2.4 Vacuum alignment

Let us now consider the A_4 triplet fields ϕ which also carry Z_5 charges. In the full model there are four such triplet fields, or "flavons", denoted as ϕ_1^u, ϕ_2^u, ϕ_1^d, ϕ_2^d. The idea is that ϕ_i^u are responsible for up-type quark flavour, while ϕ_i^d are responsible for down-type quark flavour. These VEVs are driven by the superpotential terms,

$$g_{21}P_{21}(\phi_2^u\phi_1^d \pm M_{21}^2) + g_{12}P_{12}(\phi_1^u\phi_2^d \pm M_{12}^2) + P_{ii}\left(g_{ii}^u\frac{(\phi_i^u)^5}{\Lambda^3} + g_{ii}^d\frac{(\phi_i^d)^5}{\Lambda^3} \pm M_{ii}^2\right), \quad (2.10)$$

where P_{ij} are linear combinations of singlets as in [34]. The coupling constants g_{ij}, mass parameters M_{ij} and cut-off scale Λ are enforced to be real by CP while the fields ϕ_i^u and ϕ_i^d will develop VEVs with quantised phases. If we assume that ϕ_i^u both have the same phase, $e^{im\pi/5}$, then eq. (2.10) implies that ϕ_i^d should have phases $e^{in\pi/5}$ such that

$$\arg(\phi_i^u) = \frac{m\pi}{5}, \qquad \arg(\phi_i^d) = \frac{n\pi}{5}, \qquad n+m = 0 \pmod 5, \quad (2.11)$$

where n, m are positive or negative integers.

The structure of the Yukawa matrices depends on the so-called CSD4 vacuum alignments of these flavons which were first derived in [34], and we assume a similar set of alignments here, although here the overall phases are quantised due to Z_5,

$$\langle\phi_1^u\rangle = \frac{V_1^u}{\sqrt{2}}e^{im\pi/5}\begin{pmatrix}0\\1\\1\end{pmatrix}, \qquad \langle\phi_2^u\rangle = \frac{V_2^u}{\sqrt{21}}e^{im\pi/5}\begin{pmatrix}1\\4\\2\end{pmatrix}, \quad (2.12)$$

and

$$\langle\phi_1^d\rangle = V_1^d e^{in\pi/5}\begin{pmatrix}1\\0\\0\end{pmatrix}, \qquad \langle\phi_2^d\rangle = V_2^d e^{in\pi/5}\begin{pmatrix}0\\1\\0\end{pmatrix}. \quad (2.13)$$

We note here that the vacuum alignments in eq. (2.13) and the first alignment in eq. (2.12) are fairly "standard" alignments that are encountered in tri-bimaximal mixing models, while the second alignment in eq. (2.12) is obtained using orthogonality arguments, as discussed in [34], to which we refer the interested reader for more details.

2.5 Two light Higgs doublets

The model will involve Higgs bi-doublets of two kinds, h_u which lead to up-type quark and neutrino Yukawa couplings and h_d which lead to down-type quark and charged lepton Yukawa couplings. In addition a Higgs bidoublet h_3, which is also an A_4 triplet, is used to give the third family Yukawa couplings.

After the PS and A_4 breaking, most of these Higgs bi-doublets will get high scale masses and will not appear in the low energy spectrum. In fact only two light Higgs doublets will survive down to the TeV scale, namely H_u and H_d. The precise mechanism responsible for this is quite intricate and is discussed in appendix B. Analogous Higgs mixing mechanisms are implicitly assumed in many models, but are rarely discussed explicitly (however for an example within SO(10) see [52]).

JHEP08(2014)130

The basic idea is that the light Higgs doublet H_u with hypercharge $Y = +1/2$, which couples to up-type quarks and neutrinos, is a linear combination of components of the Higgs bi-doublets of the kind h_u and h_3, while the light Higgs doublet H_d with hypercharge $Y = -1/2$, which couples to down-type quarks and charged leptons, is a linear combination of components of Higgs bi-doublets of the kind h_d and h_3,

$$h_u, h_3 \to H_u, \qquad h_d, h_3 \to H_d. \tag{2.14}$$

2.6 Yukawa operators

The renormalisable Yukawa operators, which respect PS and A_4 symmetries, have the following form, leading to the third family Yukawa couplings shown, using eqs. (2.2), (2.14),

$$F.h_3 F_3^c \to Q_3 H_u u_3^c + Q_3 H_d d_3^c + L_3 H_u \nu_3^c + L_3 H_d e_3^c, \tag{2.15}$$

where we have used eqs. (2.2), (2.14). The non-renormalisable operators, which respect PS and A_4 symmetries, have the following form,

$$F.\phi_i^u h_u F_i^c \to Q.\langle\phi_i^u\rangle H_u u_i^c + L.\langle\phi_i^u\rangle H_u \nu_i^c, \tag{2.16}$$

$$F.\phi_i^d h_d F_i^c \to Q.\langle\phi_i^d\rangle H_d d_i^c + L.\langle\phi_i^d\rangle H_d e_i^c, \tag{2.17}$$

where $i = 1$ gives the first column of each Yukawa matrix, while $i = 2$ gives the second column and we have used eqs. (2.2), (2.14). Thus the third family masses are naturally larger since they correspond to renormalisable operators, while the hierarchy between first and second families arises from a hierarchy of flavon VEVs.

2.7 Yukawa matrices

Inserting the vacuum alignments in eqs. (2.12) and (2.13) into eqs. (2.16) and (2.17), together with the renormalisable third family couplings in eq. (2.15), gives the Yukawa matrices of the form,

$$Y^u = Y^\nu = \begin{pmatrix} 0 & b & 0 \\ a & 4b & 0 \\ a & 2b & c \end{pmatrix}, \qquad Y^d \sim Y^e \sim \begin{pmatrix} y_d^0 & 0 & 0 \\ 0 & y_s^0 & 0 \\ 0 & 0 & y_b^0 \end{pmatrix}. \tag{2.18}$$

The PS unification predicts the equality of Yukawa matrices $Y^u = Y^\nu$ and $Y^d \sim Y^e$, while the A_4 vacuum alignment predicts the structure of each Yukawa matrix, essentially identifying the first two columns with the vacuum alignments in eqs. (2.12) and (2.13). With a diagonal right-handed Majorana mass matrix, Y^ν leads to a successful prediction of the PMNS mixing parameters [34]. Also the Cabibbo angle is given by $\theta_C \approx 1/4$ [35]. Thus eq. (2.18) is a good starting point for a theory of quark and lepton masses and mixing, although the other quark mixing angles and the quark CP phase are approximately zero. However above discussion ignores the effect of Clebsch factors which will alter the relationship between elements of Y^d and Y^e, which also include off-diagonal elements responsible for small quark mixing angles in the full model.

JHEP08(2014)130

name	field	$\mathrm{SU}(4)_C \times \mathrm{SU}(2)_L \times \mathrm{SU}(2)_R$	A_4	Z_5	R
Quarks	F	$(4,2,1)$	3	1	1
and leptons	$F^c_{1,2,3}$	$(\overline{4},1,2)$	1	α,α^3,1	1
PS Higgs	$\overline{H^c}$, H^c	$(4,1,2)$, $(\overline{4},1,2)$	1	1	0
A_4 triplet	$\phi^u_{1,2}$	$(1,1,1)$	3	α^4,α^2	0
flavons	$\phi^d_{1,2}$	$(1,1,1)$	3	α^3,α	0
	h_3	$(1,2,2)$	3	1	0
Higgs	h_u	$(1,2,2)$	$1''$	α	0
bidoublets	h_d,h^d_{15}	$(1,2,2)$, $(15,2,2)$	$1'$	α^3,α^4	0
	h^u_{15}	$(15,2,2)$	1	α	0
Dynamical	Σ_u	$(1,1,1)$	$1''$	α	0
masses	Σ_d,Σ^d_{15}	$(1,1,1)$, $(15,1,1)$	$1'$	α^3,α^2	0
Majoron	ξ	$(1,1,1)$	1	α^4	0
	$X_{F''_{1,3}}$	$(4,2,1)$	$1''$	α,α^3	1
Fermion	$X_{F'_{1,3}}$	$(4,2,1)$	$1'$	α,α^3	1
Messengers	$X_{\overline{F_i}}$	$(\overline{4},2,1)$	1	α^i	1
	X_{ξ_i}	$(1,1,1)$	1	α^i	1

Table 1. The basic Higgs, matter, flavon and messenger content of the model, where $\alpha = e^{2\pi i/5}$ under Z_5. R is a supersymmetric R-symmetry.

3 The model

The most important fields appearing in the model are defined in table 1. In addition to the fields introduced in the previous overview, the full model involves Higgs bi-doublets h_{15} in the adjoint of $\mathrm{SU}(4)_C$, as well as messenger fields X with masses given by the VEV of dynamical fields Σ. The effective non-renormalisable Yukawa operators therefore arise from a renormalisable high energy theory, where heavy messengers X with dynamical masses $\langle\Sigma\rangle$ are integrated out, below the energy scale $\langle\Sigma\rangle$.

3.1 Operators from messengers

Although the Yukawa operators in the up sector of the full model turn out to be the same as in eq. (2.16), the Yukawa operators in the down sector of the full model will involve Clebsch factors which will imply that Y^d and Y^e are not equal. In addition Y^d and Y^e will involve off-diagonal elements which however are "very small" in the sense that they will give rise to the small quark mixing angles of order V_{ub} and V_{cb}. The Cabibbo angle arises predominantly from the second column of Y^u, with the prediction $V_{us} \sim 1/4$ being corrected by the very small off-diagonal elements of Y^d.

The allowed Yukawa operators arise from integrating out heavy fermion fields called "messengers" and will depend on the precise choice of fermion messengers. In table 1

JHEP08(2014)130

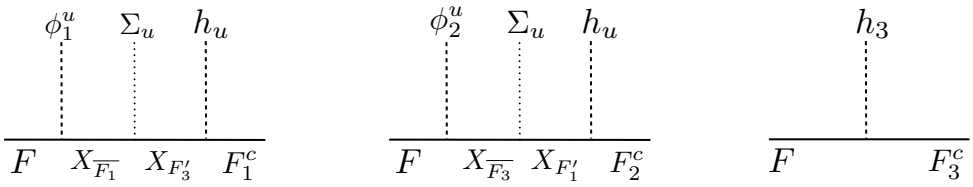

Figure 2. The fermion messenger diagrams responsible for the operators leading to the up type quark and Dirac neutrino masses. The fermions depicted by the solid line have even R-parity.

we have allowed messengers of the form $X_{\overline{F}_i}$ for charges α^i $(i = 1, \ldots, 4)$, with a very restricted set of messengers $X_{F_1'}$ $(X_{F_1''})$ and $X_{F_3'}$ $(X_{F_3''})$ with charges α and α^3, in the $1'$ $(1'')$ representation of A_4.

The assumed messengers $X_{\overline{F}_i}$ have allowed couplings to ϕF as follows,

$$X_{\overline{F}_1}\phi_1^u F + X_{\overline{F}_2}\phi_1^d F + X_{\overline{F}_3}\phi_2^u F + X_{\overline{F}_4}\phi_2^d F. \tag{3.1}$$

The messengers $X_{F'}$ and $X_{F''}$ have allowed couplings to hF_i^c as follows,

$$X_{F_1'}h_u F_2^c + X_{F_3'}h_u F_1^c + X_{F_1''}h_d F_1^c + X_{F_1''}h_{15}^d F_3^c + X_{F_3''}h_{15}^d F_2^c. \tag{3.2}$$

The messengers couple to each other and become heavy via the dynamical mass fields Σ which appear in table 1,

$$X_{F_1'}\Sigma_u X_{\overline{F}_3} + X_{F_3'}\Sigma_u X_{\overline{F}_1} + X_{F_1''}(\Sigma_d X_{\overline{F}_1} + \Sigma_{15}^d X_{\overline{F}_2}) + X_{F_3''}\Sigma_d X_{\overline{F}_4}. \tag{3.3}$$

The leading order operators responsible for the Yukawa couplings involving the first and second families to Higgs fields are obtained by integrating out the heavy messengers, leading to effective operators.

The diagrams in figure 2 yield the following operators which will be responsible for the up-type quark and neutrino Yukawa couplings,

$$W_{Yuk}^u = F.\frac{\phi_1^u}{\Sigma_u}h_u F_1^c + F.\frac{\phi_2^u}{\Sigma_u}h_u F_2^c + F.h_3 F_3^c. \tag{3.4}$$

The above operators are similar to those in eq. (2.16) and will yield a Yukawa matrix $Y^u = Y^\nu$ as in eq. (2.18).

The diagrams in figure 3 yield the operators which will be responsible for the diagonal down-type quark and charged lepton Yukawa couplings,

$$W_{Yuk}^{d,\text{diag}} = F.\frac{\phi_1^d}{\Sigma_{15}^d}h_d F_1^c + F.\frac{\phi_2^d}{\Sigma_d}h_{15}^d F_2^c + F.h_3 F_3^c. \tag{3.5}$$

These operators are similar to those in eq. (2.17) and will yield Yukawa matrices similar to those in eq. (2.18) but with $Y^d \neq Y^e$ due to the Clebsch-Gordan coefficients from the Higgs in the 15 dimensional representation of $\text{SU}(4)_C$. In addition, the above messenger sector generates further effective operators which give rise to off-diagonal down-type quark and charged lepton Yukawa couplings,

$$W_{Yuk}^{d,\text{off}-\text{diag}} = F.\frac{\phi_1^d}{\Sigma_{15}^d}h_{15}^d F_3^c + F.\frac{\phi_1^u}{\Sigma_d}(h_d F_1^c + h_{15}^d F_3^c). \tag{3.6}$$

JHEP08(2014)130

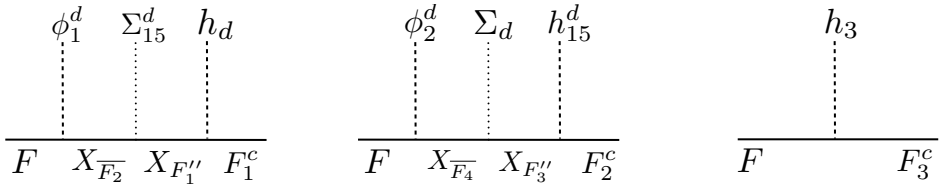

Figure 3. The fermion messenger diagrams responsible for the operators which lead to the diagonal charged lepton and down type quark masses. The fermions depicted by the solid line have even R-parity.

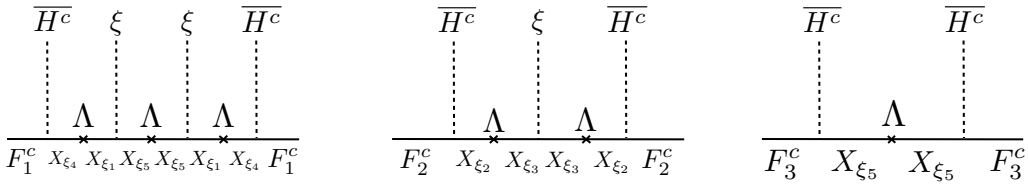

Figure 4. The fermion messenger diagrams responsible for the effective operators in eq. (3.7) leading to the diagonal heavy (right-handed) Majorana neutrino masses. The fermions depicted by the solid line have even R-parity.

The operators responsible for the heavy Majorana neutrino masses are given by,

$$W_{Maj} = \frac{\xi^2}{\Lambda^2}\frac{\overline{H^c H^c}}{\Lambda}F_1^c F_1^c + \frac{\xi}{\Lambda}\frac{\overline{H^c H^c}}{\Lambda}F_2^c F_2^c + \frac{\xi}{\Lambda}\frac{\overline{H^c H^c}}{\Lambda}F_1^c F_3^c + \frac{\overline{H^c H^c}}{\Lambda}F_3^c F_3^c, \tag{3.7}$$

corresponding to the diagrams in figure 4. These operators are mediated by the singlet messengers X_{ξ_i} and involve the explicit messenger mass scale Λ which may take values higher than the $A_4 \times Z_5$ and Pati-Salam breaking scales. The first three of these operators are controlled by the Majoron fields ξ_i in table 1, which carries a non-trivial phase due to the Z_5 symmetry, as discussed later.

Note that the dynamical mass Σ fields do not enter the Majorana sector since they transform under A_4 as $1', 1''$ and hence do not couple to pairs of X_{ξ_i}. Also note that the Majoron ξ fields which transform under $A_4 \times Z_5$ as $\xi \sim (1, \alpha^4)$ do not enter the charged fermion sector since they do not couple $X_{\overline{F}_i}$ to the messengers $X_{F'}$ and $X_{F''}$ which transform under A_4 as $1'$ and $1''$.

3.2 Yukawa and Majorana mass matrices

According to the mechanism discussed in appendix B, the four Higgs multiplets in the fourth block of table 1, h_3, h_u, h_d, h_{15}^d, result in two low energy light Higgs doublets H_u,H_d,

$$h_3 \to H_{u,d}, \quad h_u \to \epsilon_u H_u, \quad h_d \to \epsilon_d H_d, \quad h_{15}^d \to H_d, \tag{3.8}$$

where H_u is predominantly composed of the Higgs doublet from third component of h_3 with a small admixture ϵ_u of the Higgs doublet from h_u. H_d is predominantly composed of the Higgs doublet from h_{15}^d plus the third component of h_3, together with a small admixture ϵ_d of the Higgs doublet from h_d. The particular admixtures assumed in eq. (3.8) correspond to a particular choice of masses in appendix B.

JHEP08(2014)130

With the vacuum alignments in eq. (2.12), the operators in eq. (3.4) then result in non-diagonal and equal up-type quark and neutrino Yukawa matrices,

$$Y^u = Y^\nu = \begin{pmatrix} 0 & b & 0 \\ a & 4b & 0 \\ a & 2b & c \end{pmatrix}, \tag{3.9}$$

where,

$$a \sim \epsilon_u \frac{V_1^u}{\langle \Sigma_u \rangle}, \qquad b \sim \epsilon_u \frac{V_2^u}{\langle \Sigma_u \rangle}, \qquad c \sim 1. \tag{3.10}$$

Note that since $Y^u = Y^\nu$, the up-type quark masses are equal to the Dirac neutrino masses,

$$m_u = m_{\nu 1}^D, \qquad m_c = m_{\nu 2}^D, \qquad m_t = m_{\nu 3}^D. \tag{3.11}$$

From eq. (3.9) the up-type quark masses are given to excellent approximation by,

$$m_u = y_u v_u = a v_u/\sqrt{17}, \qquad m_c = y_c v_u = \sqrt{17} b v_u, \qquad m_t = c v_u. \tag{3.12}$$

The Yukawa coupling eigenvalues for up-type quarks are given by,

$$y_u \sim \frac{a}{\sqrt{34}} \sim 4.10^{-6}, \qquad y_c \sim b\sqrt{\frac{17}{21}} \sim 10^{-3}, \qquad y_t \sim c \sim 1, \tag{3.13}$$

where we have inserted some typical up-type quark Yukawa couplings, hence,

$$a \sim 2.10^{-5}, \qquad b \sim 10^{-3} \longrightarrow \frac{a}{b} \sim \frac{V_1^u}{V_2^u} \sim 2.10^{-2}, \tag{3.14}$$

where the ratio of up to charm masses is accounted for by the 2% ratio of flavon VEVs.

Similarly, with the vacuum alignments in eqs. (2.12), (2.13), the operators in eqs. (3.5), (3.6) then result in down-type quark and charged lepton Yukawa matrices related by Clebsch factors,

$$Y^d = \begin{pmatrix} y_d^0 & 0 & A y_d^0 \\ B y_d^0 & y_s^0 & C y_d^0 \\ B y_d^0 & 0 & y_b^0 + C y_d^0 \end{pmatrix}, \qquad Y^e = \begin{pmatrix} -y_d^0/3 & 0 & A y_d^0 \\ B y_d^0 & -3 y_s^0 & -3 C y_d^0 \\ B y_d^0 & 0 & y_b^0 - 3 C y_d^0 \delta \end{pmatrix}, \tag{3.15}$$

where the diagonal Yukawa couplings for down-type quarks are given by,

$$y_d^0 \sim \epsilon_d \frac{V_1^d}{\langle \Sigma_{15}^d \rangle} \sim 5.10^{-5}, \qquad y_s^0 \sim \frac{V_2^d}{\langle \Sigma_d \rangle} \sim 10^{-3}, \qquad y_b^0 \sim 5.10^{-2}, \tag{3.16}$$

where $\epsilon_{u,d}$ were defined in eq. (3.8) and for low $\tan\beta$ we have inserted some typical down-type quark Yukawa couplings, assuming that the mixing angles are small. The off-diagonal entries to the down-type quark and charged lepton Yukawa matrices are given by,

$$A y_d^0 \sim \frac{V_1^d}{\langle \Sigma_{15}^d \rangle}, \qquad B y_d^0 \sim \epsilon_d \frac{V_1^u}{\langle \Sigma_d \rangle}, \qquad C y_d^0 \sim \frac{V_1^u}{\langle \Sigma_d \rangle}, \tag{3.17}$$

JHEP08(2014)130

where,

$$A \sim \frac{C}{B} \sim \frac{1}{\epsilon_d}. \tag{3.18}$$

From eq. (3.15) the diagonal down-type quark and charged lepton Yukawa couplings are related by,

$$y_e^0 = \frac{y_d^0}{3}, \qquad y_\mu^0 = 3y_s^0, \qquad y_\tau^0 = y_b^0. \tag{3.19}$$

These are the well-known Georgi-Jarlskog (GJ) relations [53], although the factor of 1/3 which appears in the first relation above arises from a new mechanism, namely due to non-singlet fields which appear in the denominator of effective operators as discussed in detail in [54]. The viablity of the GJ relations for mass eigenstates is discussed in [5, 6]. However here there are small off-diagonal entries in the Yukawa matrices which will provide corrections to the mass eigenstates, as well as other corrections to the GJ relations, as discussed later.

Finally, from eq. (3.7), we find the heavy Majorana mass matrix,

$$M_R = \begin{pmatrix} M_1 & 0 & M_{13} \\ 0 & M_2 & 0 \\ M_{13} & 0 & M_3 \end{pmatrix}. \tag{3.20}$$

The heavy Majorana neutrino masses from eq. (3.7) are in the ratios,

$$M_1 : M_2 : M_3 \sim \tilde{\xi}^2 : \tilde{\xi} : 1, \tag{3.21}$$

where,

$$\tilde{\xi} = \frac{\langle \xi \rangle}{\Lambda}. \tag{3.22}$$

There is a competing correction to M_1 coming from the off-diagonal element, namely $M_{13}^2/M_3 \sim \tilde{\xi}^2$ with the same phase, which may be absorbed into the definition of the lightest right-handed neutrino mass. Since we need to have a strong hierarchy of right-handed neutrino masses we shall require (see later),

$$M_1 \sim 5.10^5 \text{ GeV}, \qquad M_2 \sim 5.10^{10} \text{ GeV}, \qquad M_3 \sim 5.10^{15} \text{ GeV}, \tag{3.23}$$

which may be achieved for example by,

$$\tilde{\xi} \sim 10^{-5}. \tag{3.24}$$

Typically the heaviest right-handed neutrino mass is given by,

$$M_3 \sim \frac{\langle \overline{H^c} \rangle^2}{\Lambda} \sim 5.10^{15} \text{ GeV}, \tag{3.25}$$

which is within an order of magnitude of the Pati-Salam breaking scale in eq. (2.5). This implies that $\Lambda \sim 5.10^{16}$ GeV and hence, from eq. (3.24),

$$\langle \xi \rangle \sim 5.10^{11} \text{GeV}. \tag{3.26}$$

The Majoron fields ξ act like a dynamical mass for M_2, with an effective coupling $\xi N_2^c N_2^c$ with a coupling constant of about 0.1. In principle they could play a role in leptogenesis. For example, the effect of Majorons on right-handed neutrino annihilations, leading to possibly significantly enhanced efficiency factors, was recently discussed in [55].

JHEP08(2014)130

4 Quark masses and mixing

4.1 Convention

We shall use the convention for the quark Yukawa matrices,

$$\mathcal{L} = -v^u Y^u_{ij} \overline{u}^i_{\rm L} u^j_{\rm R} - v^d Y^d_{ij} \overline{d}^i_{\rm L} d^j_{\rm R} + h.c. \tag{4.1}$$

which are diagonalised by,

$$U_{u_{\rm L}}\, Y^u\, U^\dagger_{u_{\rm R}} = \begin{pmatrix} y_u & 0 & 0 \\ 0 & y_c & 0 \\ 0 & 0 & y_t \end{pmatrix}, \qquad U_{d_{\rm L}}\, Y^d\, U^\dagger_{d_{\rm R}} = \begin{pmatrix} y_d & 0 & 0 \\ 0 & y_s & 0 \\ 0 & 0 & y_b \end{pmatrix}. \tag{4.2}$$

The CKM matrix is then given by,

$$U_{\rm CKM} = U_{u_{\rm L}} U^\dagger_{d_{\rm L}}. \tag{4.3}$$

In the PDG parameterization [56], in the standard notation, $U_{\rm CKM} = R^q_{23} U^q_{13} R^q_{12}$ in terms of $s^q_{ij} = \sin(\theta^q_{ij})$ and $c^q_{ij} = \cos(\theta^q_{ij})$ and the CP violating phase δ^q.

4.2 Analytic estimates for quark mixing

In the above convention, the quark Yukawa matrices differ from those given in eqs. (3.9), (3.15) by a complex conjugation,[2]

$$Y^u = \begin{pmatrix} 0 & b & 0 \\ a & 4b & 0 \\ a & 2b & c \end{pmatrix}, \qquad Y^d = \begin{pmatrix} y^0_d & 0 & Ay^0_d \\ By^0_d & y^0_s & Cy^0_d \\ By^0_d & 0 & y^0_b + Cy^0_d \end{pmatrix}, \tag{4.4}$$

where the parameters defined in eqs. (3.13), (3.16), 3.17 are given below,

$$a \sim \epsilon_u e^{-im\pi/5} \frac{V^u_1}{\langle \Sigma_u \rangle} \sim 2.10^{-5}, \quad b \sim \epsilon_u e^{-im\pi/5} \frac{V^u_2}{\langle \Sigma_u \rangle} \sim 10^{-3}, \quad c \sim 1, \tag{4.5}$$

$$y^0_d \sim \epsilon_d e^{-in\pi/5} \frac{V^d_1}{\langle \Sigma^d_{15} \rangle} \sim 5.10^{-5}, \quad y^0_s \sim e^{-in\pi/5} \frac{V^d_2}{\langle \Sigma_d \rangle} \sim 10^{-3}, \quad y^0_b \sim 5.10^{-2}, \tag{4.6}$$

$$Ay^0_d \sim e^{-in\pi/5} \frac{V^d_1}{\langle \Sigma^d_{15} \rangle}, \qquad By^0_d \sim \epsilon_d e^{-im\pi/5} \frac{V^u_1}{\langle \Sigma_d \rangle}, \qquad Cy^0_d \sim e^{-im\pi/5} \frac{V^u_1}{\langle \Sigma_d \rangle}, \tag{4.7}$$

where we have displayed the phases from eqs. (2.12), (2.13) explicitly in the new convention.

Cabibbo mixing clearly arises predominantly from the up-type quark Yukawa matrix Y^u, which leads to a Cabibbo angle $\theta_C \approx 1/4$ or $\theta_C \approx 14^\circ$. The other quark mixing angles and CP violating phase arise from the off-diagonal elements of Y^d, which also serve to correct the Cabibbo angle to yield eventually $\theta_C \approx 13^\circ$.

[2] The complex conjugation of the Yukawa matrices arises from the fact that the Yukawa matrices given in eqs. (3.9), (3.15) correspond to the Lagrangian $\mathcal{L} = -v^u Y^u_{ij} u^i_{\rm L} u^c_j - v^d Y^d_{ij} d^i_{\rm L} d^c_j + h.c.$ involving the unbarred left-handed and CP conjugated right-handed fields. Note that our LR convention for the quark Yukawa matrices in eq. (4.1) differs by an Hermitian conjugation compared to that used in the Mixing Parameter Tools package [57] due to the RL convention used there.

JHEP08(2014)130

Recall that any 3×3 unitary matrix $U^\dagger$ can be written in terms of three angles θ_{ij}, three phases δ_{ij} (in all cases $i<j$) and three phases ρ_i in the form [24],

$$U^\dagger = U_{23}U_{13}U_{12}\,\mathrm{diag}(e^{i\rho_1}, e^{i\rho_2}, e^{i\rho_3})\ , \tag{4.8}$$

where

$$U_{12} = \begin{pmatrix} c_{12} & s_{12}e^{-i\delta_{12}} & 0 \\ -s_{12}e^{i\delta_{12}} & c_{12} & 0 \\ 0 & 0 & 1 \end{pmatrix} \tag{4.9}$$

and similarly for U_{13}, U_{23}, where $s_{ij} = \sin\theta_{ij}$ and $c_{ij} = \cos\theta_{ij}$ and the angles can be made positive by a suitable choice of the δ_{ij} phases. We use this parameterisation for both $U^\dagger_{u_L}$ and $U^\dagger_{d_L}$, where the phases ρ_i can be absorbed into the quark mass eigenstates, leaving

$$U^\dagger_{u_L} = U^{u_L}_{23}U^{u_L}_{13}U^{u_L}_{12}\ , \qquad U^\dagger_{d_L} = U^{d_L}_{23}U^{d_L}_{13}U^{d_L}_{12}\,, \tag{4.10}$$

where $U^\dagger_{u_L}$ contains θ^u_{ij} and δ^u_{ij}, while $U^\dagger_{d_L}$ contains θ^d_{ij} and δ^d_{ij}. The CKM matrix before phase removal may be written as

$$U'_{\rm CKM} = U^{u_L}_{12}{}^\dagger U^{u_L}_{13}{}^\dagger U^{u_L}_{23}{}^\dagger U^{d_L}_{23}U^{d_L}_{13}U^{d_L}_{12}\ . \tag{4.11}$$

On the other hand, $U'_{\rm CKM}$ can be also parametrised as in eq. (4.8),

$$U'_{\rm CKM} = \mathrm{diag}(e^{i\rho_1}, e^{i\rho_2}, e^{i\rho_3})\,U_{23}U_{13}U_{12}\ . \tag{4.12}$$

The angles θ_{ij} are the standard PDG ones in U_{CKM}, and five of the six phases of $U'_{\rm CKM}$ in eq. (4.12) may be removed leaving the standard PDG phase in $U_{\rm CKM}$ identified as [24]:

$$\delta^q = \delta^q_{13} - \delta^q_{23} - \delta^q_{12}. \tag{4.13}$$

In the present case, given Y^u, it is clear that $\theta^u_{13} \approx \theta^u_{23} \approx 0$. Similary, given Y^d, we see that $\theta^d_{12} \approx 0$. This implies that eq. (4.11) simplifies to:

$$U'_{\rm CKM} \approx U^{u_L}_{12}{}^\dagger U^{d_L}_{23}U^{d_L}_{13}\ . \tag{4.14}$$

Then, by equating the right-hand sides of eqs. (4.12) and (4.14) and expanding to leading order in the small mixing angles, we obtain the following relations:

$$\theta^q_{23}e^{-i\delta^q_{23}} \approx \theta^d_{23}e^{-i\delta^d_{23}}\ , \tag{4.15}$$

$$\theta^q_{13}e^{-i\delta^q_{13}} \approx \theta^d_{13}e^{-i\delta^d_{13}} - \theta^u_{12}e^{-i\delta^u_{12}}\theta^d_{23}e^{-i\delta^d_{23}}\ , \tag{4.16}$$

$$\theta^q_{12}e^{-i\delta^q_{12}} \approx -\theta^u_{12}e^{-i\delta^u_{12}}\ , \tag{4.17}$$

from which we deduce,

$$\theta^q_{12} \approx \theta^u_{12}, \qquad \theta^q_{23} \approx \theta^d_{23}, \qquad |\theta^q_{13} - \theta^q_{12}\theta^q_{23}e^{i\delta^q}| \approx \theta^d_{13}, \tag{4.18}$$

where,

$$\theta^u_{12} \sim \frac{1}{4}, \qquad \theta^d_{23} \sim \left|\frac{Cy^0_d}{y^0_b}\right|, \qquad \theta^d_{13} \sim \left|\frac{Ay^0_d}{y^0_b}\right|. \tag{4.19}$$

JHEP08(2014)130

Notice from eqs. (4.18), (4.19) that the magnitudes of the Yukawa matrix elements are all approximately fixed in terms of physical quark mixing parameters,

$$\theta^q_{23} \sim \left|\frac{Cy^0_d}{y^0_b}\right| \sim 0.040, \qquad |\theta^q_{13} - \theta^q_{12}\theta^q_{23}e^{i\delta^q}| \sim \left|\frac{Ay^0_d}{y^0_b}\right| \sim 0.009. \tag{4.20}$$

Since $|y^0_d/y^0_b| \sim 0.001$, eq. (4.20) implies that,

$$A \sim 9, \qquad C \sim 40, \qquad B \sim C/A \sim 4, \tag{4.21}$$

where the last relation uses eq. (3.18).

Concerning the phases, from eq. (4.7) we find, in the convention of eq. (4.9),

$$\delta^u_{12} \sim 0, \qquad \delta^d_{23} \sim -\arg\left(\frac{Cy^0_d}{y^0_b}\right) \sim m\pi/5, \qquad \delta^d_{13} \sim -\arg\left(\frac{Ay^0_d}{y^0_b}\right) \sim n\pi/5, \tag{4.22}$$

where, from eq. (2.11), $n+m$ is a multiple of 5. Hence, from eqs. (4.15), (4.16), 4.17,

$$\delta^q_{12} \sim 0, \qquad \delta^q_{23} \sim \delta^d_{23} \sim m\pi/5, \qquad \delta^q_{13} \sim -\arg\left(0.009e^{-in\pi/5} - \frac{1}{4}0.04e^{-im\pi/5}\right), \tag{4.23}$$

so the physical CP phase is given by the very approximate expression,

$$\delta^q = \delta^q_{13} - \delta^q_{23} - \delta^q_{12} \sim -\arg(0.009e^{-in\pi/5} - 0.010e^{-im\pi/5}) - \frac{m\pi}{5}. \tag{4.24}$$

Clearly CP violation requires $n \neq m$, indeed δ^q only depends on the difference $n-m$ with a positive value of $\delta^q \sim \frac{7\pi}{18}$ in the first quadrant requiring $n < m$. Since $n+m$ must be a multiple of 5, then the only possibility is $n = 2, m = 3$ which corresponds to one of the discrete choices of phases in eq. (2.11).

4.3 Numerical results for quark mixing

With the phases fixed by the choice of discrete choice of phases $n = 2, m = 3$, as discussed in the previous subsection, the only free parameters are a, b, c in the up sector, and A, B, C and y^0_d, y^0_s, y^0_b in the down sector matrices, where we have explicitly removed the phases from these parameters, in order to make them real,

$$Y^u = \begin{pmatrix} 0 & be^{-i3\pi/5} & \epsilon c \\ ae^{-i3\pi/5} & 4be^{-i3\pi/5} & 0 \\ ae^{-i3\pi/5} & 2be^{-i3\pi/5} & c \end{pmatrix}. \tag{4.25}$$

$$Y^d = \begin{pmatrix} y^0_d e^{-i2\pi/5} & 0 & Ay^0_d e^{-i2\pi/5} \\ By^0_d e^{-i3\pi/5} & y^0_s e^{-i2\pi/5} & Cy^0_d e^{-i3\pi/5} \\ By^0_d e^{-i3\pi/5} & 0 & y^0_b + Cy^0_d e^{-i3\pi/5} \end{pmatrix} \tag{4.26}$$

Note that we have introduced a small correction term ϵ in the $(1,3)$ entry of Y^u which will mainly affect θ^q_{13}. Physically this corresponds to a small admixture of the first component of the Higgs triplet h_3 contributing to the physical light Higgs state H_u, as discussed in

JHEP08(2014)130

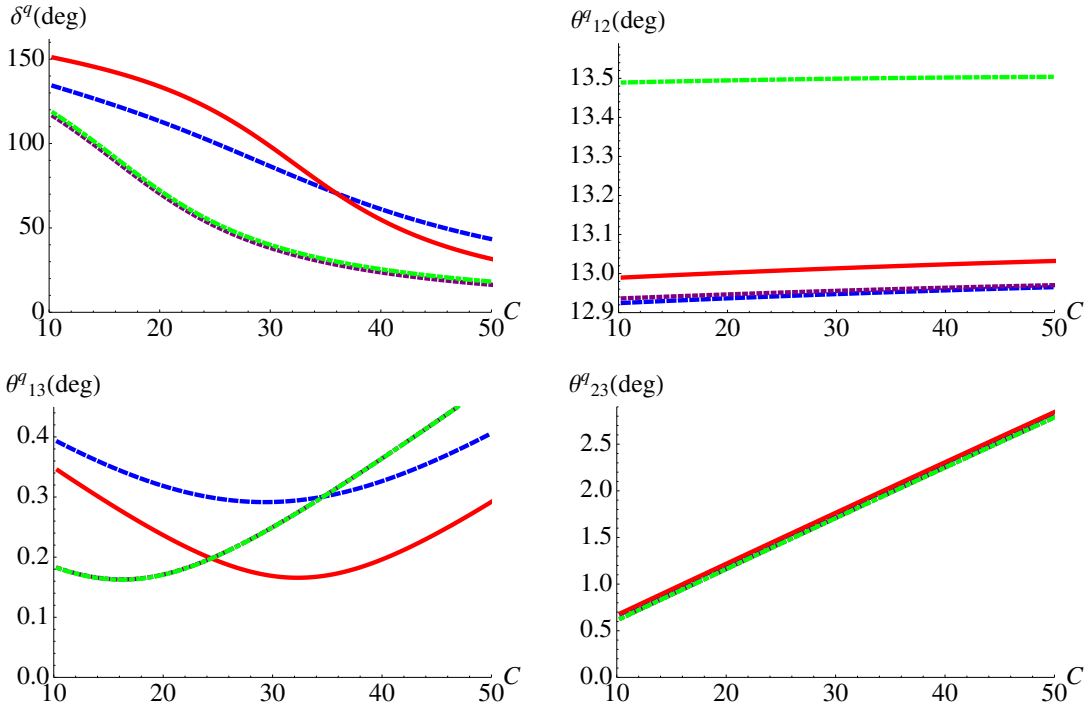

Figure 5. CKM parameters resulting from eqs. (4.25), (4.26), all plotted in degrees as a function of C, using the parameters in eqs. (4.27), (4.28). Green dot dashed lines are for $A = 5, B = 3$ with $\epsilon = 0$. Purple dotted lines are for $A = 5, B = 7$ with $\epsilon = 0$. Blue dashed lines are for $A = 9, B = 7$ with $\epsilon = 0$. Red solid lines are for $A = 9, B = 7$ with $\epsilon = -2.4 \times 10^{-3}$.

appendix B. The previous analytic results were for $\epsilon = 0$, but we find numerically that the best fit to CKM parameters requires a non-zero value of ϵ.

For the following results, we shall fix the parameters which approximately determine the six quark masses at the high scale to be,

$$a = 1.6.10^{-5}, \qquad b = 0.8.10^{-3}, \qquad c = 0.75, \tag{4.27}$$

$$y_d^0 = 0.9.10^{-5}, \qquad y_s^0 = 1.4.10^{-4}, \qquad y_b^0 = -0.9.10^{-2}, \tag{4.28}$$

Although the quark results are insensitive to the sign of y_b^0, the lepton sector results lead to a better fit with the negative sign of y_b^0 as discussed later. Using the Mixing Parameter Tools (MPT) package [57], in figure 5 we show the CKM parameters for different choices of A, B as a function of C. θ_{23}^q is really only sensitive to C only, while θ_{12}^q is mainly sensitive to B. θ_{13}^q and δ^q are both sensitive A. The effect of the correction ϵ is to shift the blue dashed curve to the red solid curve, lowering θ_{13}^q while leaving θ_{23}^q almost unchanged, allowing the best fit of the CKM parameters for $C = 36$.

To take a concrete example, for the red solid at the value $C = 36$, with the above input parameters $A = 9, B = 7$ (cf. eq. (4.21)) and $\epsilon = -2.4 \times 10^{-3}$, we find the quark Yukawa eigenvalues at the high scale,

$$y_u = 3.9.10^{-6}, \qquad y_c = 3.3.10^{-3}, \qquad y_t = 0.75, \tag{4.29}$$

$$y_d = 0.81.10^{-5}, \qquad y_s = 1.5.10^{-4}, \qquad y_b = 0.91.10^{-2} \tag{4.30}$$

JHEP08(2014)130

and the CKM parameters at the high scale,

$$\theta_{12}^q = 13.02^\circ, \qquad \theta_{13}^q = 0.17^\circ, \qquad \theta_{23}^q = 2.09^\circ, \qquad \delta^q = 70.4^\circ. \tag{4.31}$$

These parameters are consistent with those given, for example, in [5, 6], after including RG corrections, in particular due to the large top Yukawa coupling. Notice that there are as many input parameters as there are physical observables in the quark sector, so no prediction is claimed. However we emphasise two interesting features, firstly that the Cabibbo angle is understood to arise from Y^u leading to $\theta_C \approx 1/4$ or $\theta_C \approx 14^0$, with a small (one degree) correction mainly controlled by B. Secondly the phases which appear are quantised according to Z_5, which also controls the leptonic phases as discussed in the following subsection. Indeed, with $Y^\nu = Y^u$ fixed by the quark sector, the entire neutrino sector only depends on three additional right-handed neutrino masses, which determine the three physical neutrino masses, with the entire neutrino mixing matrix then being fully determined, with only very small charged lepton mixing corrections appearing in the PMNS mixing matrix.

5 Lepton masses and mixing

In this section we discuss the leading order predictions for PMNS mixing which arise from the neutrino Yukawa and Majorana matrices in eq. (3.9) which result in a very simple form of effective neutrino mass matrix, after the see-saw mechanism has been applied.

5.1 Convention

The neutrino Yukawa matrix Y^ν is defined in a LR convention by[3]

$$\mathcal{L} = -v^u Y^\nu_{\alpha i} \overline{\nu}^\alpha_{\rm L} \nu^i_{\rm R} + h.c.$$

where $\alpha = e, \mu, \tau$ labels the three left-handed neutrinos and $i = 1, 2, 3$ labels the three right-handed neutrinos.

The physical effective neutrino Majorana mass matrix m^ν is determined from the columns of Y^ν via the see-saw mechanism,

$$m^\nu = -v_u^2 \, Y^\nu M_{\rm R}^{-1} Y^{\nu T} \, , \tag{5.1}$$

where the light Majorana neutrino mass matrix m^ν is defined by[4] $\mathcal{L}_\nu = -\frac{1}{2} m^\nu \overline{\nu}_{\rm L} \nu^c_{\rm L} +$ h.c., while the heavy right-handed Majorana neutrino mass matrix M_R is defined by $\mathcal{L}^R_\nu = -\frac{1}{2} M_R \overline{\nu}^c_{\rm R} \nu_{\rm R} +$ h.c. and m^ν is diagonalised by

$$U_{\nu_{\rm L}} \, m^\nu \, U^T_{\nu_{\rm L}} = \begin{pmatrix} m_1 & 0 & 0 \\ 0 & m_2 & 0 \\ 0 & 0 & m_3 \end{pmatrix}. \tag{5.2}$$

[3] This LR convention for the Yukawa matrix differs by an Hermitian conjugation compared to that used in the Mixing Parameter Tools package [57] due to the RL convention used there.

[4] Note that this convention for the light effective Majorana neutrino mass matrix m^ν differs by an overall complex conjugation compared to that used in the Mixing Parameter Tools package [57].

JHEP08(2014)130

The PMNS matrix is then given by

$$U_{\rm PMNS} = U_{e_{\rm L}} U^\dagger_{\nu_{\rm L}} \ . \tag{5.3}$$

We use a standard parameterization $U_{\rm PMNS} = R^l_{23} U^l_{13} R^l_{12} P^l$ in terms of $s^l_{ij} = \sin(\theta^l_{ij})$, $c^l_{ij} = \cos(\theta^l_{ij})$, the Dirac CP violating phase δ^l and further Majorana phases contained in $P^l = {\rm diag}(e^{i\frac{\beta^l_1}{2}}, e^{i\frac{\beta^l_2}{2}}, 1)$. The standard PDG parameterization [56] differs slightly due to the definition of Majorana phases which are by given by $P^l_{\rm PDG} = {\rm diag}(1, e^{i\frac{\alpha_{21}}{2}}, e^{i\frac{\alpha_{31}}{2}})$. Evidently the PDG Majorana phases are related to those in our convention by $\alpha_{21} = \beta^l_2 - \beta^l_1$ and $\alpha_{31} = -\beta^l_1$, after an overall unphysical phase is absorbed by $U_{e_{\rm L}}$.

5.2 See-saw mechanism

The neutrino Yukawa and Majorana matrices are as in eq. (3.9), with $Y^\nu = Y^u$ in eq. (4.25),

$$Y^\nu = \begin{pmatrix} 0 & be^{-i3\pi/5} & 0 \\ ae^{-i3\pi/5} & 4be^{-i3\pi/5} & 0 \\ ae^{-i3\pi/5} & 2be^{-i3\pi/5} & c \end{pmatrix}, \qquad M_R \approx \begin{pmatrix} M_1 e^{8i\pi/5} & 0 & 0 \\ 0 & M_2 e^{4i\pi/5} & 0 \\ 0 & 0 & M_3 \end{pmatrix}, \tag{5.4}$$

where we have ignored the small off-diagonal Majorana mass M_{13} which gives a tiny mixing correction of order 10^{-5} from eq. (3.24), and dropped the correction ϵ which is completely negligible in the lepton sector due to sequential dominance (see below). We have also assumed a phase in the Majoron VEV $\langle\xi\rangle \sim e^{4i\pi/5}$ in the operators in eq. (3.7) responsible for the right-handed neutrino masses, as discussed below.

Using eq. (5.4), the see-saw formula in eq. (5.1) leads to the neutrino mass matrix m^ν,

$$m^\nu = m_a \begin{pmatrix} 0&0&0 \\ 0&1&1 \\ 0&1&1 \end{pmatrix} + m_b e^{2i\eta} \begin{pmatrix} 1&4&2 \\ 4&16&8 \\ 2&8&4 \end{pmatrix} + m_c e^{2i\eta} \begin{pmatrix} 0&0&0 \\ 0&0&0 \\ 0&0&1 \end{pmatrix}, \tag{5.5}$$

where,

$$m_a = \frac{a^2 v_u^2}{M_1}, \ m_b = \frac{b^2 v_u^2}{M_2}, \ m_c = \frac{c^2 v_u^2}{M_3}, \tag{5.6}$$

are three real parameter combinations which determine the three physical neutrino masses m_1, m_2, m_3, respectively. According to sequential dominance m_c will determine the lightest neutrino mass m_1 where we will have $m_1 \ll m_2 < m_3$, so that the third term arising from the heaviest right-handed neutrino of mass M_3 is approximately decoupled from the see-saw mechanism. (This is why the correction ϵ is completely negligible in the lepton sector.)

In order to understand the origin of the relative phases $\eta = 2\pi/5$ which enter the neutrino mass matrix m^ν, it is worth recalling that the see-saw operators responsible for the dominant first two terms of the neutrino mass matrix in eq. (5.5) have the form

$$m^\nu \sim \frac{\langle\phi_{\rm atm}\rangle\langle\phi_{\rm atm}\rangle^T}{\langle\xi\rangle^2} + \frac{\langle\phi_{\rm sol}\rangle\langle\phi_{\rm sol}\rangle^T}{\langle\xi\rangle}, \tag{5.7}$$

where we have written $\phi_{\rm atm} = \phi^u_1$, $\phi_{\rm sol} = \phi^u_2$ to highlight the fact that the first term gives the dominant contribution to the atmospheric neutrino mass m_3, while the second

JHEP08(2014)130

term controls the solar neutrino mass m_2. The mild neutrino hierarchy between m_3 and m_2 emerges due to the choice of Majoron VEV $\langle\xi\rangle$ in eq. (3.24) which partly cancels the hierarchy in the square of the flavon VEVs in eq. (3.14). The lightest neutrino mass m_1 arises from smaller terms (not shown), leading to a normal neutrino mass hierarchy, where the heaviest atmospheric neutrino mass m_3 is associated with the lightest right-handed neutrino mass M_1 as in light sequential dominance [21–23].

Since $\langle\phi_{\rm atm}\rangle$ and $\langle\phi_{\rm sol}\rangle$ have the same phase, $e^{-i3\pi/5}$, and $\langle\xi\rangle$ has a phase[5] $e^{4i\pi/5}$, eq. (5.7) shows that the atmospheric term has a phase $(e^{-i3\pi/5})^2/(e^{4i\pi/5})^2 = e^{-14i\pi/5}$, while the solar term is real. After multiplying m^ν by an overall phase $e^{4i\pi/5}$, which we are allowed to do since overall phases are irrelevant, the atmospheric term becomes real, while the other two terms pick up phases of $e^{4i\pi/5}$. This is equivalent to having a phase $\eta = 2\pi/5$ in eq. (5.5). Different choices of phase for η are theoretically possible, but the phenomenologically successful choice for the relative phase of the atmospheric and solar terms (the first and second terms in eq. (5.5)) is $\eta = 2\pi/5$, whereas for example $\eta = -2\pi/5$ leaves the mixing angles unchanged but reverses the sign of the CP phases [33–35]. The dependence on see-saw phases was fully discussed in [33]. Here we only note that in this model the see-saw phases are restricted to a discrete choice corresponding to the fifth roots of unity due to the Z_5 symmetry. The fact that the decoupled third term proportional to m_c (responsible for the lightest neutrino mass m_1) has the same phase as the second term proportional to m_b (responsible for the solar neutrino mass) is a new prediction of the current model and will affect the m_1 dependence of the results.

From eqs. (3.11), (3.12), the Dirac neutrino masses are equal to the up-type quark masses which are related to a, b, y_t and hence eq. (5.6) becomes,

$$m_a = 17\frac{m_u^2}{M_1}, \quad m_b = \frac{m_c^2}{17M_2}, \quad m_c = \frac{m_t^2}{M_3}. \tag{5.8}$$

Using eq. (5.8), the three right-handed neutrino masses M_1, M_2, M_3 may be determined for particular values of m_a, m_b, m_c, and the known quark masses m_u, m_c, m_t (evaluated at high scales).

The neutrino mass matrix in eq. (5.5) may be diagonalised numerically to determine the physical neutrino masses and the PMNS mixing matrix as in eq. (5.2). We emphasise that, at leading order, with the phase $\eta = 2\pi/5$ fixed by the previous argument, the neutrino mass matrix involves just 3 real input parameters m_a, m_b, m_c from which 12 physical parameters in the lepton sector are predicted, comprising 9 lepton parameters from diagonalising the neutrino mass matrix m^ν in eq. (5.5) (the 3 angles θ^l_{ij}, 3 phases $\delta^l, \beta^l_1, \beta^l_2$ and the 3 light neutrino masses m_i) together with the 3 heavy right-handed neutrino masses M_i from eq. (5.8). The model is clearly highly predictive, involving 12 predictions in the lepton sector from only 3 input parameters.

[5] This phase is the complex conjugate of the phase given in the previous convention in eq. (3.7).

JHEP08(2014)130

5.3 A first numerical example

To take a numerical example, diagonalising the neutrino mass matrix in eq. (5.5), with the three input parameters

$$m_a = 0.035 \text{ eV}, \quad m_b = 0.002 \text{ eV}, \quad m_c = 0.002 \text{ eV}, \tag{5.9}$$

the Mixing Parameter Tools package [57] gives the physical neutrino masses,

$$m_1 = 3.29.10^{-4} \text{ eV}, \quad m_2 = 8.62.10^{-3} \text{ eV}, \quad m_3 = 4.93.10^{-2} \text{ eV}, \tag{5.10}$$

corresponding to the mass squared differences,

$$\Delta m^2_{21} = 7.42.10^{-5} \text{ eV}^2, \quad \Delta m^2_{31} = 2.43.10^{-3} \text{ eV}^2, \quad \Delta m^2_{32} = 2.36.10^{-3} \text{ eV}^2, \tag{5.11}$$

and the lepton mixing parameters,

$$\theta^l_{12} = 32.2^\circ, \quad \theta^l_{13} = 9.3^\circ, \quad \theta^l_{23} = 41.6^\circ, \quad \delta^l = 248^\circ, \quad \beta^l_1 = 114^\circ, \quad \beta^l_2 = 90^\circ. \tag{5.12}$$

The PDG Majorana phases [56] are given by $\alpha_{21} = \beta^l_2 - \beta^l_1$ and $\alpha_{31} = -\beta^l_1$. For the choice of input parameters in eq. (5.9) and the high scale quark masses,

$$m_u = 1 \text{ MeV}, \quad m_c = 400 \text{ MeV}, \quad m_t = 100 \text{ GeV}, \tag{5.13}$$

eq. (5.8) then determines the three right-handed neutrino masses to be,

$$M_1 = 5 \times 10^5 \text{ GeV}, \quad M_2 = 5 \times 10^9 \text{ GeV}, \quad M_3 = 5 \times 10^{15} \text{ GeV}. \tag{5.14}$$

eq. (5.9) shows the 3 input parameters, while eqs. (5.10), (5.12), 5.14 shows the 12 output predictions. One may regard the 3 input parameters in eq. (5.9) as fixing the 3 light physical neutrino masses in eq. (5.10), with all the 6 PMNS matrix parameters in eq. (5.12) as being independent predictions, along with the 3 right-handed neutrino masses in eq. (5.14).

So far we have ignored charged lepton corrections which are expected in the model to be small. However the corrections are not entirely negligible as the following example shows. The charged lepton Yukawa matrix is given from eq. (3.15),

$$Y^e = \begin{pmatrix} -(y^0_d/3)e^{-i2\pi/5} & 0 & Ay^0_d e^{-i2\pi/5} \\ By^0_d e^{-i3\pi/5} & -3y^0_s e^{-i2\pi/5} & -3Cy^0_d e^{-i3\pi/5} \\ By^0_d e^{-i3\pi/5} & 0 & y^0_b - 3Cy^0_d e^{-i3\pi/5} \end{pmatrix}. \tag{5.15}$$

which should be compared to the down quark Yukawa matrix in eq. (4.26). The off-diagonal elements of Y^e are small, similar to those of Y^d which are responsible for the small quark mixing angles and a correction to the Cabibbo angle of one degree. The quark mixing angles fix the three real parameters to be for example $A = 9, B = 7, C = 36$ and the down quark couplings in eq. (4.28). Including the charged lepton Yukawa matrix with these parameters and the same neutrino mass parameters as in eq. (5.9), the MPT package gives the lepton mixing parameters,

$$\theta^l_{12} = 32.15^\circ, \quad \theta^l_{13} = 8.9^\circ, \quad \theta^l_{23} = 45.2^\circ, \quad \delta^l = 259^\circ, \quad \beta^l_1 = 92^\circ, \quad \beta^l_2 = 70^\circ. \tag{5.16}$$

JHEP08(2014)130

Comparing the results in eq. (5.16) to those in eq. (5.12), we see that the atmospheric angle has increased by about 3° to become maximal due to the (2, 3) element in the charged lepton Yukawa matrix, which is enhanced by a Clebsch factor of 3 relative to the same element in the down Yukawa matrix. The reactor angle has decreased slightly, and the CP oscillation phase has increased. With y_b^0 taken to be positive instead of negative, and all the other parameters unchanged, we find the results below,

$$\theta_{12}^l = 32.27°, \quad \theta_{13}^l = 9.65°, \quad \theta_{23}^l = 37.3°, \quad \delta^l = 240°, \quad \beta_1^l = 132°, \quad \beta_2^l = 106°. \quad (5.17)$$

The main effect of the sign of y_b^0 is on the atmospheric and reactor angles.

5.4 Modified Georgi-Jarlskog relations

Since the charged lepton masses are known with much higher precision than the down type quark masses, the down Yukawa couplings in practice will be predicted from inputting the charged lepton masses in order to accurately fix y_d^0, y_s^0, y_b^0. Comparing Y^e in eq. (5.15) to Y^d in eq. (4.26), we find that we do not get exactly the GJ relations in eq. (3.19) due to the off-diagonal elements which also involve Clebsch factors. Numerically we find that, for y_b^0 negative and the other parameters as above, the Yukawa eigenvalues at the GUT scale are approximately related as,

$$y_e = \frac{y_d}{2.6}, \qquad y_\mu = 2.8 y_s, \qquad y_\tau = 0.97 y_b, \quad (5.18)$$

while for y_b^0 positive we find,

$$y_e = \frac{y_d}{3.0}, \qquad y_\mu = 2.7 y_s, \qquad y_\tau = 1.05 y_b. \quad (5.19)$$

These may be compared to the phenomenological relation [5, 6],

$$\left| \frac{y_\mu}{y_s} \frac{y_d}{y_e} \right| = 10.7^{+1.8}_{-0.8}. \quad (5.20)$$

For example for y_b^0 negative we find the r.h.s. to be 7.3 which differs by more than 4 sigma. In order to bring this relation into better agreement with experiment we would need to increase this ratio, for example by increasing the muon Yukawa eignenvalue compared to the strange quark Yukawa eigenvalue. One way to do this is to introduce a flavon ϕ_2^{d15} with the same charges as ϕ_2^d but in the adjoint 15 of $SU(4)_C$. The middle diagram in figure 3 involving ϕ_2^{d15} involves a Clebsch factor of +9 as compared to the factor of -3 with ϕ_2^d [54]. Below the PS the colour singlet component of ϕ_2^{d15} mixes with ϕ_2^d, to yield a light flavon combination,

$$\phi_2^{d'} = \phi_2^{d15} \cos\gamma + \sin\gamma \phi_2^d. \quad (5.21)$$

Hence middle diagram in figure 3 involving $\phi_2^{d'}$ implies the relation,

$$\frac{y_\mu^0}{y_s^0} = 9\cos\gamma - 3\sin\gamma. \quad (5.22)$$

JHEP08(2014)130

For example by suitable choice of the mixing angle γ we can arrange $y^0_\mu = 4.5 y^0_s$,

$$Y^e = \begin{pmatrix} -(y^0_d/3)e^{-i2\pi/5} & 0 & A y^0_d e^{-i2\pi/5} \\ B y^0_d e^{-i3\pi/5} & -4.5 y^0_s e^{-i2\pi/5} & -3C y^0_d e^{-i3\pi/5} \\ B y^0_d e^{-i3\pi/5} & 0 & y^0_b - 3C y^0_d e^{-i3\pi/5} \end{pmatrix}. \tag{5.23}$$

By comparing Y^e in eq. (5.23) to Y^d in eq. (4.26), we find the modified GJ relations,

$$y_e = \frac{y_d}{2.6}, \qquad y_\mu = 4.1 y_s, \qquad y_\tau = 0.97 y_b, \tag{5.24}$$

and hence,

$$\left| \frac{y_\mu}{y_s} \frac{y_d}{y_e} \right| = 10.7, \tag{5.25}$$

which reproduces the central value in eq. (5.20). In the above estimate we have assumed $A = 9, B = 7, C = 36$ and the other couplings in eq. (4.28). Using the same neutrino mass parameters as in eq. (5.9), the MPT package gives the same lepton mixing parameters as for the GJ form in eq. (5.16), to very good accuracy.

5.5 Numerical results for neutrino masses and lepton mixing

In our numerical results we shall use the charged lepton Yukawa matrix in eq. (5.23), together with the neutrino mass matrix in eq. (5.5), as summarised below,

$$m^\nu = m_a \begin{pmatrix} 0 & 0 & 0 \\ 0 & 1 & 1 \\ 0 & 1 & 1 \end{pmatrix} + m_b e^{i4\pi/5} \begin{pmatrix} 1 & 4 & 2 \\ 4 & 16 & 8 \\ 2 & 8 & 4 \end{pmatrix} + m_c e^{i4\pi/5} \begin{pmatrix} 0 & 0 & 0 \\ 0 & 0 & 0 \\ 0 & 0 & 1 \end{pmatrix}, \tag{5.26}$$

$$Y^e = \begin{pmatrix} -(y^0_d/3)e^{-i2\pi/5} & 0 & A y^0_d e^{-i2\pi/5} \\ B y^0_d e^{-i3\pi/5} & -4.5 y^0_s e^{-i2\pi/5} & -3C y^0_d e^{-i3\pi/5} \\ B y^0_d e^{-i3\pi/5} & 0 & y^0_b - 3C y^0_d e^{-i3\pi/5} \end{pmatrix}. \tag{5.27}$$

As discussed previously, the lepton mixing depends on predominantly on m^ν which involves the three real mass parameters m_a, m_b, m_c, which are effectively fixed by the neutrino masses. However there are small corrections coming from Y^e, which involves the real parameters A, B, C which determine the quark mixing angles and the real Yukawa couplings y^0_d, y^0_s, y^0_b which were previously determined from the down-type quark masses.

As discussed previously (cf. eqs. (5.12), (5.16), 5.17) the effect on lepton mixing depends on the sign of y^0_b where the negative sign pushes up the atmospheric angle towards maximal, while also decreasing the reactor angle, while the positive sign has the opposite effect. Here we shall show results for the negative sign of y^0_b, as in eq. (4.28). We shall also use the same real parameters $A = 9, B = 7, C = 36$ which gave a good fit to the quark mixing angles and CP phase in eq. (4.31). Since lepton mixing depends mainly on the three real mass parameters m_a, m_b and m_c which also determine the neutrino masses, we shall show results as a function of the neutrino mass parameters. Here we shall restrict ourselves to showing results where we keep the parameters appearing in Y^e fixed at the above "benchmark" values, and vary only m_a, m_b and m_c. The parameter m_a is mainly responsible for the

JHEP08(2014)130

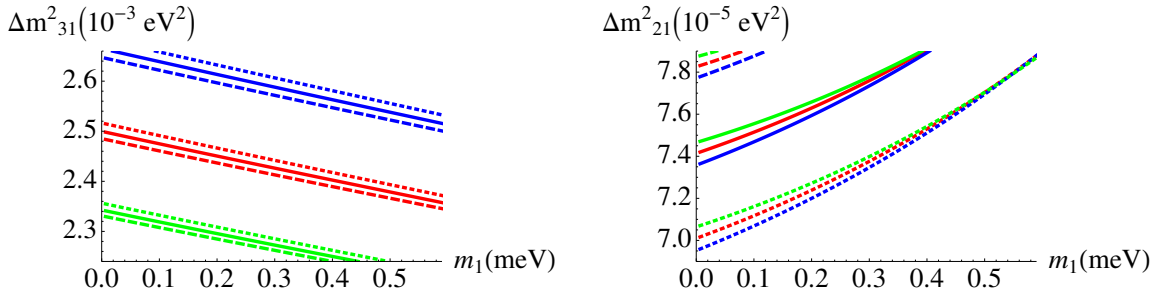

Figure 6. The neutrino mass squared parameters Δm^2_{31} and Δm^2_{21} resulting from eq. (5.26), plotted as a function of the lightest neutrino mass m_1. Each line corresponds to a fixed m_a and m_b with varied m_c. The (Blue, Red, Green) coloured lines correspond to $m_a = (0.036, 0.035, 0.034)\,\text{eV}$, respectively, and give (High, Central, Low) values of Δm^2_{31}. The (Dashed, Solid, Dotted) styles correspond to $m_b = (0.00210, 0.00205, 0.00200)\,\text{eV}$, respectively, and yield (High, Central, Low) values of Δm^2_{21}. The parameter m_c is varied from $0 - 0.004\,\text{eV}$ corresponding to $m_1 = 0 - 0.006\,\text{eV}$.

atmospheric neutrino mass and hence Δm^2_{31}, while m_b is mainly responsible for the solar neutrino mass and hence Δm^2_{21}, with m_c being mainly responsible for the lightest neutrino mass m_1, which is zero for $m_c = 0$. Once the parameters m_a and m_b are chosen to fix Δm^2_{31} and Δm^2_{21} for $m_c = 0$, then all neutrino parameters are predicted as a function of m_c and hence m_1, as described below.

Using the Mixing Parameter Tools package [57], in figure 6 we show the neutrino mass squared differences as a function of the lightest physical neutrino mass m_1, corresponding to varying m_c for various fixed values of m_a, m_b as given in the figure caption. Note that Δm^2_{21} actually increases with m_1. This is because, with fixed m_a and m_b, switching on m_c also increases m_2. Since m_2^2 increases linearly with m_c, after expanding, this has a more significant effect on Δm^2_{21} than the quadratic increase of m_1^2, in the region of small m_c. In figure 7 we show the resulting model predictions for the lepton mixing angles and CP oscillation phase. In all the plots (blue, red, green) coloured lines correspond to (high, central, low) values of Δm^2_{31}, while the (dashed, solid, dotted) styles correspond to (high, central, low) values of Δm^2_{21}. Note that the presently 3σ allowed range of mass squared parameters are [12, 13]: $\Delta m^2_{31} = (2.25 - 2.65).10^{-3}\,\text{eV}^2$, $\Delta m^2_{21} = (7.0 - 8.0).10^{-5}\,\text{eV}^2$, and our choice of parameters covers most of these ranges. Thus the red solid curve corresponds to central values of both Δm^2_{31} and Δm^2_{21} for low values of m_1, while the other curves reflect the uncertainty in the PMNS predictions due to the present precision in the neutrino mass squared differences.

Using the Mixing Parameter Tools package [57], in figure 7 we show the PMNS predictions of the model, resulting from eqs. (5.26), (5.27), plotted as a function of the lightest neutrino mass m_1. From figure 7, the PMNS parameters are predicted to be in the following ranges:

$$\theta^l_{12} = 34^\circ - 31^\circ, \quad \theta^l_{13} = 8.4^\circ - 9.7^\circ, \quad \theta^l_{23} = 44.4^\circ - 46.4^\circ, \quad \delta^l = 266^\circ - 256^\circ. \tag{5.28}$$

These predictions should be compared to the presently 3σ allowed ranges:

$$\theta^l_{12} = 31^\circ - 36^\circ, \quad \theta^l_{13} = 5.5^\circ - 10^\circ, \quad \theta^l_{23} = 37^\circ - 55^\circ, \quad \delta^l = 0^\circ - 360^\circ, \tag{5.29}$$

JHEP08(2014)130

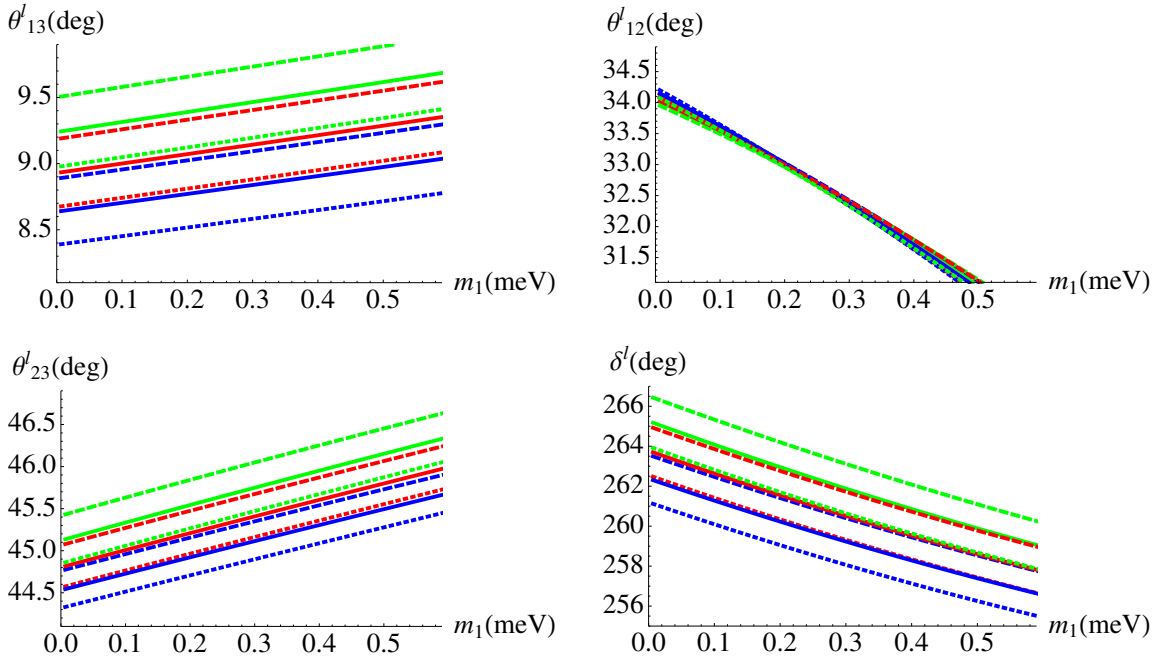

Figure 7. PMNS predictions of the model, resulting from eqs. (5.26), (5.27), plotted as a function of the lightest neutrino mass m_1 for charged lepton parameters given by $A = 9, B = 7, C = 36$ and the down quark couplings in eq. (4.28). Each line corresponds to a fixed m_a and m_b with varied m_c, using the same values as in figure 6, with the colour coding and line styles as before.

and the best fit values for a normal hierarchy with 1σ errors [11]:

$$\theta^l_{12} = 34.63^\circ{}^{+1.02^\circ}_{-0.98^\circ}, \quad \theta^l_{13} = 8.80^\circ{}^{+0.37^\circ}_{-0.39^\circ}, \quad \theta^l_{23} = 48.9^\circ{}^{+1.6^\circ}_{-7.4^\circ}, \quad \delta^l = 241^\circ{}^{+115^\circ}_{-68^\circ}. \tag{5.30}$$

The solar angle prediction is $34^\circ \gtrsim \theta^l_{12} \gtrsim 31^\circ$, for the lightest neutrino mass in the range $0 \lesssim m_1 \lesssim 0.5$ meV, corresponding to a normal neutrino mass hierarchy. Since the solar angle is very insensitive to Δm^2_{31} and Δm^2_{21} values, and decreases as m_1 increases, an accurate determination of the solar angle will accurately determine m_1 in this model. The model also predicts a reactor angle $\theta^l_{13} = 9^\circ \pm 0.5^\circ$, close to its best fit value, with a significant dependence on Δm^2_{31} and Δm^2_{21}. A striking prediction of the model is the atmospheric angle which is predicted to be close to maximal to within about one degree for nearly all allowed Δm^2_{31} and Δm^2_{21}. The bulk of the parameter space for low m_1 predicts in fact $\theta^l_{23} = 45^\circ \pm 0.5^\circ$. It is worth noting that the most recent fit [11] is quite compatible with maximal atmospheric mixing to within 1σ for the case of a normal mass squared ordering, when the latest T2K disappearance data is included. The model also predicts accurately the CP phase with the bulk of the parameter space around $\delta^l = 260^\circ \pm 5^\circ$, compatible with the best fit value, although the latter has a much larger error.

In general one can expect corrections coming from renormalisation group (RG) running [58, 59] as well as canonical normalisation corrections [60–62]. For a SUSY GUT with light sequential dominance, as in the present model, the RG corrections for high $\tan\beta \sim 50$ have been shown to be [59]: $\Delta\theta^l_{23} \sim +1^\circ$, $\Delta\theta^l_{12} \sim +0.4^\circ$, $\Delta\theta^l_{13} \sim -0.1^\circ$, where the positive

JHEP08(2014)130

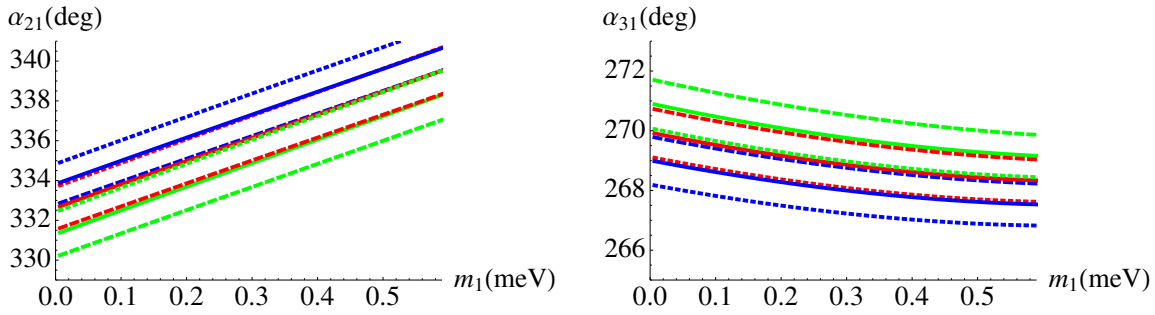

Figure 8. Majorana phases (in PDG convention defined below eq. (5.3)) as predicted by the model, resulting from eqs. (5.26), (5.27), plotted as a function of the lightest neutrino mass m_1 for charged lepton parameters given by $A = 9, B = 7, C = 36$ and the down quark couplings in eq. (4.28). Each line corresponds to a fixed m_a and m_b with varied m_c, using the same values as in figure 6, with the colour coding and line styles as before.

sign means that the value increases in running from the GUT scale to low energy, while for low $\tan\beta \lesssim 10$ the RG corrections are negligible compared to the range of the predictions. In particular the effect of right-handed neutrino thresholds [58] is expected to be negligible in this model since the heaviest right-handed neutrino mass is close to the GUT scale, while the lighter right-handed neutrinos have very small Yukawa couplings given by $a \sim 2.10^{-5}$ and $b \sim 10^{-3}$ from eq. (3.14).

We emphasise that, since the parameters in Y^e in eq. (5.27) are fixed from the quark sector, and the light neutrino masses are determined by three real parameters m_a, m_b, m_c in eq. (5.26), the entire PMNS matrix containing 3 mixing angles and 3 CP phases emerges as a prediction of the model, although 2 of these CP phases will be difficult to measure for a normal neutrino mass hierarchy, so we have not plotted their predictions. The model may be tested most readily by its prediction of maximal atmospheric mixing and a normal neutrino mass hierarchy. It would be interesting to perform a χ^2 analysis of the quark and lepton masses and mixing angles predicted by the model, but that is beyond the scope of the present paper.

5.6 Majorana phases, neutrinoless double beta decay and sum of neutrino masses relevant for cosmology

The Majorana phases α_{21}, α_{31} (in PDG convention defined below eq. (5.3)) predicted by the model are displayed in figure 8, using the same parameter sets and colour coding as for the other plots. Note that $\alpha_{31} \approx -90°$, similar to the oscillation phase δ^l.

The Majorana phases α_{21}, α_{31} enter the effective mass $|m_{ee}|$ observable in neutrinoless double beta decay parameter given by,

$$|m_{ee}| = |m_1 c_{12}^2 c_{13}^2 + m_2 s_{12}^2 c_{13}^2 e^{i\alpha_{21}} + m_3 s_{13}^2 e^{i(\alpha_{31}-2\delta)}|. \tag{5.31}$$

In the present model $|m_{ee}|$ is predicted to be always very small and unobservable in the foreseeable future. For example, for the parameters in eq. (5.9), (5.10) and (5.16), we find,

$$|m_{ee}| \approx |0.2 + 2.4e^{-i0.12\pi} + 1.2e^{i0.61\pi}| \text{ meV} \approx 2.1 \text{ meV}. \tag{5.32}$$

JHEP08(2014)130

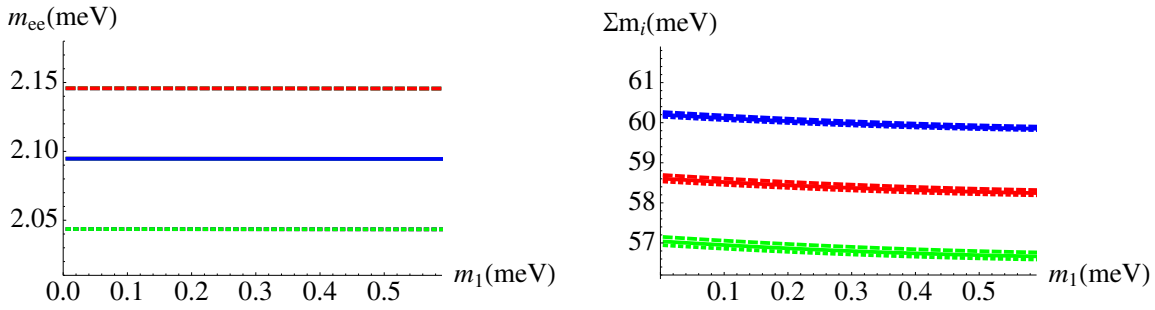

Figure 9. The neutrinoless double beta decay parameter $|m_{ee}|$ (left panel) and the sum of neutrino masses Σm_i (right panel) as predicted by the model, resulting from eqs. (5.26), (5.27), plotted as a function of the lightest neutrino mass m_1 for charged lepton parameters given by $A = 9, B = 7, C = 36$ and the down quark couplings in eq. (4.28). Each line corresponds to a fixed m_a and m_b with varied m_c, using the same values as in figure 6, with the colour coding and line styles as before.

The sum of neutrino masses is relevant for cosmology, since it contributes to hot dark matter, leading to a constraint on its value and eventually a measurement. This is defined by,

$$\Sigma m_i \equiv \Sigma_{i=1}^{3} m_i = m_1 + m_2 + m_3. \tag{5.33}$$

Due to the rather strong normal hierarchy, this value is dominated by the value of m_3, which is controlled by the parameter m_a in the neutrino mass matrix in eq. (5.26).

In figure 9 we show the neutrinoless double beta decay parameter $|m_{ee}|$ (left panel) and the sum of neutrino masses Σm_i (right panel) as predicted by the model, using the same parameter sets and colour coding as for the other plots. Note that for $|m_{ee}|$ (left panel) the three colours corresponding to different values of m_a lie accurately on top of each other. The three dashed curves predict $|m_{ee}| \approx 2.15$ meV, the three solid curves predict $|m_{ee}| \approx 2.10$ meV and the three dotted curves predict $|m_{ee}| \approx 2.05$ meV, corresponding to the three different values of $m_b = 2.15, 2.10, 2.05$. This can be understood from the neutrino mass matrix in eq. (5.26), since $|m_{ee}| = |m^{\nu}_{11}| = m_b$, with the charged lepton matrix in eq. (5.23) providing only very small corrections to this result. The fact that eq. (5.31) was used to calculate the results and agrees very accurately with the expectation $|m_{ee}| = |m^{\nu}_{11}| = m_b$ provides a highly non-trivial check on our calculation of PMNS parameters and neutrino masses, and gives confidence to all our results. Note that $|m_{ee}|$, being equal to m_b, is approximately fixed by Δm^2_{21} in figure 6. Since $|m_{ee}|$ is predicted to be too small to measure in the foreseeable future, an observation of neutrinoless double beta decay could exclude the model. Similar comments apply to a cosmological observation of Σm_i.

6 Higher order corrections

6.1 HO corrections to vacuum alignment

The triplet vacuum alignments are achieved by renormalisable superpotentials, as discussed in [34]. Since the messenger scale associated with any non-renormalisable corrections to vacuum alignment is unconstrained by the model, it is possible that any such terms may

JHEP08(2014)130

be highly suppressed. In the present analysis we shall therefore ignore any HO corrections to the vacuum alignments in eqs. (2.12), (2.13).

6.2 HO corrections to Yukawa operators

Let us now consider HO corrections to the operators in eqs. (3.4), (3.5), 3.6, consisting of extra insertions of ϕ, leading to effective operators of the type,

$$\Delta W_{Yuk} = F.\left(\frac{\phi}{\Sigma}\right)^n hF^c, \tag{6.1}$$

for $n > 1$. For example, $\frac{\phi_1^d}{\Sigma_d}$ and $\frac{\phi_2^d}{\Sigma_u}$ are both singlets of Z_5, so either of these ratios may in principle be inserted into any of the LO operators in eqs. (3.4), (3.5) 3.6. However in practice, which HO insertions are allowed will depend on the details of the messenger sector. In order for an effective operator to be allowed, it is necessary that that the messenger diagram responsible for it can be drawn, and whether this is possible or not will depend on the choice of charges of the messenger fields X_F and $X_{\overline{F}}$ under all the symmetries.

In order to allow such HO operators as in eq. (6.1), for $n > 1$, at least one of the messenger fields X_F and $X_{\overline{F}}$ would have to be a triplet of A_4 in order to permit the coupling $X_F \phi X_{\overline{F}}$ where ϕ is a triplet, as is clear from figure 10 (left panel). Such triplet messenger fields X_F and $X_{\overline{F}}$ are not required in order to construct the LO operators and must be introduced for the sole purpose of allowing the HO operators of this kind.

Moreover, such triplet messenger fields would be dangerous since they may allow operators of the kind in eq. (6.1) for $n = 1$ involving the Higgs triplet h_3 which could contribute to up and charm quark masses for example.

For these reasons we have chosen not to introduce any messenger fields X_F and $X_{\overline{F}}$ which are triplets of A_4, thereby forbidding HO operators of the type shown in eq. (6.1) for $n \geq 2$ involving any Higgs fields or involving the A_4 triplet Higgs h_3 for $n \geq 1$.

The couplings in eqs. (3.1), (3.2), 3.3 can also lead to HO operators of the generic kind, after integrating out the messengers, as shown in figure 10 (right panel).

$$\Delta W_{Yuk} = F.\left(\frac{\phi}{\Sigma}\right)\left(\frac{\Sigma}{\Sigma}\right)^n hF^c, \tag{6.2}$$

where $n \geq 1$. At the order $n = 1$, only a single operator of this kind is generated,

$$\Delta W_{Yuk} = F.\left(\frac{\phi_1^d}{\Sigma_{15}^d}\right)\left(\frac{\Sigma_d}{\Sigma_u}\right) h_u F_1^c, \tag{6.3}$$

which gives a correction in the (1,1) entry of Y^u and hence a contribution to the up quark Yukawa coupling,

$$\Delta y_u \sim \epsilon_u \frac{V_1^d}{\langle \Sigma_{15}^d \rangle}\frac{\langle \Sigma_d \rangle}{\langle \Sigma_u \rangle} \sim \frac{\epsilon_u}{\epsilon_d}\frac{\langle \Sigma_d \rangle}{\langle \Sigma_u \rangle} y_d^0, \tag{6.4}$$

where we have used y_d^0 given in eq. (3.16). The correction is small if $\epsilon_u \langle \Sigma_d \rangle \ll \epsilon_d \langle \Sigma_u \rangle$.

JHEP08(2014)130

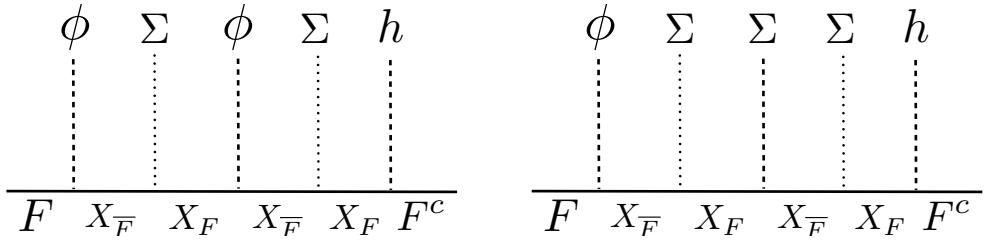

Figure 10. Some possible higher order diagrams. The left panel shows a generic diagram involving triplet fermion messengers, which if present, would lead to effective higher order operators as in eq. (6.1). In our model we assume such triplet messengers to be absent which prevents diagrams with more than one ϕ field. The right panel shows a generic diagram responsible for the effective higher order operators as in eq. (6.2).

6.3 HO corrections to Majorana operators

The relevant bilinear charges in the Majorana sector are

$$F_1^c F_1^c \sim \alpha^2, \quad F_1^c F_2^c \sim \alpha^4, \quad F_1^c F_3^c \sim \alpha, \quad F_2^c F_2^c \sim \alpha, \quad F_2^c F_3^c \sim \alpha^3, \quad F_3^c F_3^c \sim 1. \tag{6.5}$$

The messengers which transform under $A_4 \times Z_5$ as $X_{\xi_i} \sim (1, \alpha^i)$ can couple to the Majoron field $\xi \sim (1, \alpha^4)$ leading to the LO operators in eq. (3.7) (dropping $\overline{Hc}$ and Λ),

$$F_1^c F_1^c \xi^2, \qquad F_1^c F_3^c \xi, \qquad F_2^c F_2^c \xi, \qquad F_3^c F_3^c \sim 1. \tag{6.6}$$

Since each insertion of ξ carries a suppression factor of $\langle\xi\rangle/\Lambda \sim 10^{-5}$, HO operators involving more powers of ξ, such as $F_1^c F_2^c \xi^4$, are negligible.

7 Conclusions

In this paper we have proposed a rather elegant theory of flavour based on the Pati-Salam gauge group combined with $A_4 \times Z_5$ family symmetry which provides an excellent description of quark and lepton masses, mixing and CP violation. Pati-Salam unification relates quark and lepton Yukawa matrices and in particular predicts $Y^u = Y^\nu$, leading to Dirac neutrino masses being equal to up, charm and top masses. The see-saw mechanism involves very hierarchical right-handed Majorana neutrino masses with sequential dominance. The A_4 family symmetry determines the structure of Yukawa matrices via CSD4 vacuum alignment, with the three columns of $Y^u = Y^\nu$ being proportional to $(0, 1, 1)^T$, $(1, 4, 2)^T$ and $(0, 0, 1)^T$, respectively, where each column has a multiplicative phase determined by Z_5 breaking, which controls CP violation in both the quark and lepton sectors. The other Yukawa matrices $Y^d \sim Y^e$ are both approximately diagonal, with charged lepton masses related to down quark masses by modified GJ relations, and containing small off-diagonal elements responsible for the small quark mixing angles θ_{13}^q and θ_{23}^q. The model hence predicts the Cabibbo angle $\theta_C \approx 1/4$, up to such small angle corrections.

The main limitation of the model is that it does not predict the charged fermion masses. However the third family masses are naturally larger since they arise at renormalisable

JHEP08(2014)130

order, while the hierarchy between first and second family masses can be understood to originate from hierarchies between flavon VEVs. Although the model does not predict the small quark mixing angles, it does offer a qualitative understanding of both CP violation and the Cabibbo angle $\theta_C \approx 1/4$, which, as discussed above, is closely related to the lepton mixing angles via the CSD4 vacuum alignment. Moreover, the model contains 6 fewer parameters in the flavour sector than the 22 parameters of the SM, and hence predicts the entire PMNS matrix, as is clear from eqs. (5.26), (5.27) where all the parameters which appear there are fixed by fermion (including neutrino) masses and small quark mixing angles. Hence the model predicts the entire PMNS lepton mixing matrix with no free parameters, including the three lepton mixing angles and the three leptonic CP phases with negligible theoretical error from HO corrections. The resulting PMNS matrix turns out to have an approximate TBC form as regards maximal atmospheric mixing and the reactor angle $\theta^l_{13} \approx 9^\circ$, although the solar angle deviates somewhat from its tri-maximal value, corresponding to a negative deviation parameter $s \sim -0.03$ to -0.1, where $\sin\theta^l_{12} = (1+s)/\sqrt{3}$ [63].

The predictions of a normal neutrino mass hierarchy and maximal atmospheric angle will both be either confirmed or excluded over the next few years by current or near future neutrino experiments such as SuperKamiokande, T2K, NOνA and PINGU [64–68]. The Daya Bay II reactor upgrade, including the short baseline experiment JUNO [69–71], will also test the normal neutrino mass hierarchy and measure the reactor and solar angles to higher accuracy, enabling precision tests of the predictions $\theta^l_{13} = 9^\circ \pm 0.5^\circ$ and $34^\circ \gtrsim \theta^l_{12} \gtrsim 31^\circ$, for the lightest neutrino mass in the range $0 \lesssim m_1 \lesssim 0.5$ meV. With such a mass range, neutrinoless double beta decay will not be observable in the foreseeable future. In the longer term, the superbeam proposals [72] would measure the atmospheric mixing angle to high accuracy, confronting the prediction $\theta^l_{23} = 45^\circ \pm 0.5^\circ$, and ultimately testing the prediction of the leptonic CP violating oscillation phase $\delta^l = 260^\circ \pm 5^\circ$.

Acknowledgments

SFK would like to thank Pasquale Di Bari, Simon King and Christoph Luhn for discussions SFK also acknowledges partial support from the EU ITN grant INVISIBLES 289442 .

A A_4

A_4 has four irreducible representations, three singlets 1, $1'$ and $1''$ and one triplet 3. The products of singlets are:

$$1 \otimes 1 = 1 \;\; 1' \otimes 1'' = 1 \;\; 1' \otimes 1' = 1'' \;\; 1'' \otimes 1'' = 1'. \tag{A.1}$$

The generators of the A_4 group, can be written as S and T with $S^2 = T^3 = (ST)^3 = \mathcal{I}$. We work in the Ma-Rajasakaran basis [25] where the triplet generators are,

$$S = \begin{pmatrix} 1 & 0 & 0 \\ 0 & -1 & 0 \\ 0 & 0 & -1 \end{pmatrix}, \qquad T = \begin{pmatrix} 0 & 1 & 0 \\ 0 & 0 & 1 \\ 1 & 0 & 0 \end{pmatrix}. \tag{A.2}$$

In this basis one has the following Clebsch rules for the multiplication of two triplets,

$$\begin{aligned}(ab)_1 &= a_1b_1 + a_2b_2 + a_3b_3\,;\\ (ab)_{1'} &= a_1b_1 + \omega a_2b_2 + \omega^2 a_3b_3\,;\\ (ab)_{1''} &= a_1b_1 + \omega^2 a_2b_2 + \omega a_3b_3\,;\\ (ab)_{3_1} &= (a_2b_3, a_3b_1, a_1b_2)\,;\\ (ab)_{3_2} &= (a_3b_2, a_1b_3, a_2b_1)\,,\end{aligned} \tag{A.3}$$

where $\omega^3 = 1$, $a = (a_1, a_2, a_3)$ and $b = (b_1, b_2, b_3)$.

Under a CP transformation in this basis we require [44, 45],

$$a \to (a_1^*, a_3^*, a_2^*), \qquad b \to (b_1^*, b_3^*, b_2^*), \tag{A.4}$$

so that

$$\begin{aligned}(ab)_{1'} &\to a_1^*b_1^* + \omega a_3^*b_3^* + \omega^2 a_2^*b_2^* = (a^*b^*)_{1''}\\ (ab)_{1''} &\to a_1^*b_1^* + \omega^2 a_3^*b_3^* + \omega a_2^*b_2^* = (a^*b^*)_{1'}\,.\end{aligned} \tag{A.5}$$

B Two light Higgs doublets H_u and H_d

We have introduced five Higgs bi-doublet multiplets h_3, h_u, h_d, h_{15}^d, h_{15}^u, distinguished by A_4 and Z_5 charges. Ignoring $\mathrm{SU}(4)_C$ and A_4 quantum numbers, a generic Higgs bi-doublet under $\mathrm{SU}(2)_L \times \mathrm{SU}(2)_R$ may be written as

$$h = (2,2) = \begin{pmatrix} {h_1}^0 & {h_2}^+ \\ {h_1}^- & {h_2}^0 \end{pmatrix} \tag{B.1}$$

where h_1 and h_2 form two $\mathrm{SU}(2)_L$ doublets with $\mathrm{U}(1)_{T_{3R}}$ charges of $-1/2$ and $1/2$. Henceforth it is convenient to use a slightly different notation as follows. We label each of the Higgs bi-doublets as $h_a(2,2)$ and, below the $\mathrm{SU}(2)_R$ breaking scale, each of them will split into two Higgs doublets, denoted as $h_a^{\pm}(2, \pm 1/2)$ labelled by their $\mathrm{U}(1)_{T_{3R}}$ charges of $\pm 1/2$, rather than their electric charges as shown in eq. (B.1). Thus the five bi-doublets above will yield eight Higgs doublets from $h_u^{\pm}$, $h_d^{\pm}$ and the colour singlet parts of $h_{15}^{d\pm}$, $h_{15}^{u\pm}$, plus additional colour triplet and octet Higgs doublets from $h_{15}^{d\pm}$, $h_{15}^{u\pm}$, together with the six Higgs doublets from $h_3^{\pm}$. We shall arrange for nearly all of these Higgs doublets to have superheavy masses near the GUT scale, leaving only the two light Higgs doublets H_u and H_d, as follows.

The h_3 multiplet, which will be mainly responsible for the third family Yukawa couplings, is a triplet of A_4. We introduce a triplet $\phi_3 \sim 3$ which is a PS and Z_5 singlet and couples as $\phi_3 h_3 h_3$. If ϕ_3 develops a VEV in the third direction,[6] $\langle \phi_3 \rangle \sim (0, 0, V_3)$, then, using the Clebsch rules in eq. (A.5), this gives a large mass to the first two A_4 components

[6] Vacuum alignment may be achieved by a superpotential term $\zeta\phi_3\phi_3$ where ζ is an A_4 triplet driving field, leading to $\langle \phi_3 \rangle \sim (0, 0, V_3)$. In general, small corrections to this vacuum alignment can lead to $\langle \phi_3 \rangle \sim (\epsilon, 0, 1)V_3$ corresponding to a small admixture ϵ of the first component of the Higgs triplet h_3 contributing to the physical light Higgs state H_u, and hence a small correction to Y^u in eq. (4.25). Similar corrections to Y^d may be absorbed into the existing parameters in eq. (4.26).

JHEP08(2014)130

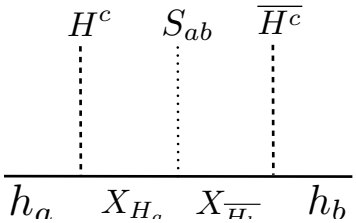

Figure 11. The diagram shows the higgsino messenger diagrams responsible for the effective operators in eqs. (B.2), (B.3) leading to GUT scale higgsino doublet masses. The higgsinos depicted by the solid line have odd R-parity.

of h_3 while leaving the third component massless. Introducing a TeV scale mass term $\mu h_3 h_3$ will give a light mass to the third component of h_3. The Higgs bi-doublets in the third A_4 component of h_3 will mix with other Higgs bi-doublets as discussed below and two linear combinations of the mixed states, H_u and H_d, will remain light, allowing the renormalisable third family Yukawa couplings.

The operators involving the Higgs fields h_u, h_d, h_{15}^d, h_{15}^u, collectively denoted as h_a, have the general form,

$$\frac{(h_a H^c)(\overline{H^c} h_b)}{S_{ab}} \to \frac{\langle H^c \rangle \langle \overline{H^c} \rangle}{\langle S_{ab} \rangle} h_a^+ h_b^- \equiv M_{ab} h_a^+ h_b^- \tag{B.2}$$

where S_{ab} are Pati-Salam singlet fields which develop VEVs somewhat higher than the Pati-Salam breaking scale. When H^c gets a VEV in its right-handed neutrino component, it will project out the $T_{3R} = +1/2$ component of h_a, which we write as h_a^+. Similarly when $\overline{H^c}$ gets a VEV in its right-handed neutrino component, it will project out the $T_{3R} = -1/2$ component of h_b, which we write as h_b^-.

The diagrams responsible for generating the operators of the form in eq. (B.2) are shown in figure 11. These diagrams should be considered as Higgsino doublet mixing diagrams. The Higgsino messenger fields which couple to $(h_a H^c)$ are denoted as X_{H_a} and those which couple to $(\overline{H^c} h_b)$ are denoted as $X_{\overline{H_b}}$, where the messenger masses are generated by the couplings $X_{H_a} S_{ab} X_{\overline{H_b}}$ when S_{ab} develops its VEV, leading to the effective operators in eq. (B.2).

The choice of singlets S_{11}, S_{33}, S_{24}, S_{34} with appropriate Z_5 and A_4 charges, lead to the following particular operators of the general form of eq. (B.2):

$$\begin{aligned} &\frac{(h_u H^c)(\overline{H^c} h_u)}{S_{11}} + \frac{(h_{15}^d H^c)(\overline{H^c} h_{15}^d)}{S_{33}} \\ &+ \frac{(h_d H^c)(\overline{H^c} h_{15}^u)}{S_{24}} + \frac{(h_{15}^u H^c)(\overline{H^c} h_d)}{S_{24}} \\ &+ \frac{(h_{15}^d H^c)(\overline{H^c} h_{15}^u)}{S_{34}} + \frac{(h_{15}^u H^c)(\overline{H^c} h_{15}^d)}{S_{34}}. \end{aligned} \tag{B.3}$$

Note that S_{ab} has the same $A_4 \times Z_5$ charges as S_{ba}.

JHEP08(2014)130

In addition we require the following three operators, involving the third component of h_3, given by $h_3.\phi_3$,

$$\frac{(\phi_3.h_3H^c)(\overline{H^c}h_u)}{\Lambda_3 S_{01}} + \frac{(h_dH^c)(\overline{H^c}h_3.\phi_3)}{\Lambda_3 S_{30}} + \frac{(h^u_{15}H^c)(\overline{H^c}h_3.\phi_3)}{\Lambda_3 S_{40}}. \tag{B.4}$$

Since the matrix of charges is symmetric (since S_{ab} has the same $A_4 \times Z_5$ charges as S_{ba}) the operators above must be given by a particular messenger sector which forbids similar operators with H^c and $\overline{H^c}$ interchanged.

The operators in eqs. (B.3), (B.4) and the term $\mu h_3 h_3$ lead to the following Higgsino mass matrix, in the basis where the rows correspond to $h_3^+, h_u^+, h_d^+, h_{15}^{d+}, h_{15}^{u+}$ and the columns correspond to $h_3^-, h_u^-, h_d^-, h_{15}^{d-}, h_{15}^{u-}$,

$$\begin{pmatrix} \mu & M_{01} & 0 & 0 & 0 \\ 0 & M_{11} & 0 & 0 & 0 \\ 0 & 0 & 0 & 0 & M_{24} \\ M_{30} & 0 & 0 & M_{33} & M_{34} \\ M_{40} & 0 & M_{42} & M_{43} & 0. \end{pmatrix}. \tag{B.5}$$

The Higgsino masses from eq. (B.5) can be written explicitly as,

$$\begin{aligned} &\mu h_3^+ h_3^- + (M_{01}h_3^+ + M_{11}h_u^+)h_u^- + h_d^+ M_{24} h_{15}^{u-} \\ &+h_{15}^{d+}(M_{30}h_3^- + M_{33}h_{15}^{d-} + M_{34}h_{15}^{u-}) \\ &+h_{15}^{u+}(M_{40}h_3^- + M_{42}h_d^- + M_{43}h_{15}^{d-}). \end{aligned} \tag{B.6}$$

By studying these mass terms it is apparent that, only one linear combination of the Higgs doublet h_u^+ and the third component of the Higgs doublet in h_3^{u+} has a large mass, namely $M_{01}h_3^+ + M_{11}h_u^+$, while the orthogonal linear combination will remain light. It is also clear that only two linear combinations of the Higgs doublet h_d^- and the colour singlet Higgs doublet in h_{15}^{d-} and the third component of the Higgs doublet in h_3^- has a large mass, while the orthogonal linear combination will remain light. By contrast, the Higgs doublets in h_u^-, h_{15}^{u-}, h_d^+, h_{15}^{d+} and h_{15}^{u+} all appear in three different terms and will all become very heavy. In particular the colour triplet and octet components of $h_{15}^{d\pm}$ will combine with those of $h_{15}^{u\mp}$ so that all coloured Higgs doublets become very massive.

In summary, most of the Higgs doublets will gain large masses near the GUT scale, leaving only two light Higgs doublets, H_u and H_d. The light Higgs doublet which couples to up-type quarks and neutrinos, H_u, will be identified as a linear combination of the third component of the Higgs doublet in h_3^{u+} and h_u^+. The light Higgs doublet, H_d, which couples to down-type quarks and charged leptons will be identified as a linear combination of the Higgs doublet h_d^-, the third component of the Higgs doublet in h_3^- and the colour singlet Higgs doublet from h_{15}^{d-}. The light mass term $\mu h_3^+ h_3^-$ will lead to the term $\mu H_u H_d$ term as in the MSSM. This term may alternatively be induced by a singlet S term $S h_3^+ h_3^-$ which will lead to the term $S H_u H_d$ term as in the NMSSM, generating a light Higgsino mass from the TeV scale singlet VEV.

JHEP08(2014)130

References

[1] ATLAS collaboration, *Observation of a new particle in the search for the Standard Model Higgs boson with the ATLAS detector at the LHC*, *Phys. Lett.* **B 716** (2012) 1 [arXiv:1207.7214] [INSPIRE].

[2] CMS collaboration, *Observation of a new boson at a mass of 125 GeV with the CMS experiment at the LHC*, *Phys. Lett.* **B 716** (2012) 30 [arXiv:1207.7235] [INSPIRE].

[3] S. Raby, *Introduction to theories of fermion masses*, hep-ph/9501349 [INSPIRE].

[4] S.F. King, *Fermion Masses and Unification*, Lectures of *Summer School on Particle Physics*, Trieste, Italy, June 11–22 2007, http://cdsagenda5.ictp.trieste.it/full_display.php?ida=a06202.

[5] S. Antusch and V. Maurer, *Running quark and lepton parameters at various scales*, *JHEP* **11** (2013) 115 [arXiv:1306.6879] [INSPIRE].

[6] G. Ross and M. Serna, *Unification and fermion mass structure*, *Phys. Lett.* **B 664** (2008) 97 [arXiv:0704.1248] [INSPIRE].

[7] A. Strumia and F. Vissani, *Neutrino masses and mixings and...*, hep-ph/0606054 [INSPIRE].

[8] S.F. King, *Neutrino mass models*, *Rept. Prog. Phys.* **67** (2004) 107 [hep-ph/0310204] [INSPIRE].

[9] Daya Bay collaboration, F.P. An et al., *Spectral measurement of electron antineutrino oscillation amplitude and frequency at Daya Bay*, *Phys. Rev. Lett.* **112** (2014) 061801 [arXiv:1310.6732] [INSPIRE].

[10] P.F. Harrison, D.H. Perkins and W.G. Scott, *Tri-bimaximal mixing and the neutrino oscillation data*, *Phys. Lett.* **B 530** (2002) 167 [hep-ph/0202074] [INSPIRE].

[11] D.V. Forero, M. Tortola and J.W.F. Valle, *Neutrino oscillations refitted*, arXiv:1405.7540 [INSPIRE].

[12] F. Capozzi, G.L. Fogli, E. Lisi, A. Marrone, D. Montanino and A. Palazzo, *Status of three-neutrino oscillation parameters, circa 2013*, *Phys. Rev.* **D 89** (2014) 093018 [arXiv:1312.2878] [INSPIRE].

[13] M.C. Gonzalez-Garcia, M. Maltoni, J. Salvado and T. Schwetz, *Global fit to three neutrino mixing: critical look at present precision*, *JHEP* **12** (2012) 123 [arXiv:1209.3023] [INSPIRE].

[14] S.F. King, *Tri-bimaximal-Cabibbo Mixing*, *Phys. Lett.* **B 718** (2012) 136 [arXiv:1205.0506] [INSPIRE].

[15] S.F. King and C. Luhn, *Neutrino Mass and Mixing with Discrete Symmetry*, *Rept. Prog. Phys.* **76** (2013) 056201 [arXiv:1301.1340] [INSPIRE].

[16] S.F. King, A. Merle, S. Morisi, Y. Shimizu and M. Tanimoto, *Neutrino Mass and Mixing: from Theory to Experiment*, *New J. Phys.* **16** (2014) 045018 [arXiv:1402.4271] [INSPIRE].

[17] P. Minkowski, $\mu \to e\gamma$ *at a Rate of One Out of 1-Billion Muon Decays?*, *Phys. Lett.* **B 67** (1977) 421 [INSPIRE].

JHEP08(2014)130

[18] T. Yanagida, in Proceedings of the *Workshop on Unified Theory and Baryon Number of the Universe*, KEK, 1979, O. Sawada and A. Sugamoto eds. pg. 95

[19] P. Ramond, *The Family Group in Grand Unified Theories*, hep-ph/9809459 [INSPIRE].

[20] M. Gell-Mann, P. Ramond and R. Slansky, in *Supergravity*, P. van Niewwenhuizen and D. Freedman eds., North Holland, Amsterdam The Netherlands (1979), *Conf. Proc.* **C790927** (1979) 315, PRINT-80-0576.

[21] S.F. King, *Atmospheric and solar neutrinos with a heavy singlet*, *Phys. Lett.* **B 439** (1998) 350 [hep-ph/9806440] [INSPIRE].

[22] S.F. King, *Atmospheric and solar neutrinos from single right-handed neutrino dominance and U(1) family symmetry*, *Nucl. Phys.* **B 562** (1999) 57 [hep-ph/9904210] [INSPIRE].

[23] S.F. King, *Large mixing angle MSW and atmospheric neutrinos from single right-handed neutrino dominance and U(1) family symmetry*, *Nucl. Phys.* **B 576** (2000) 85 [hep-ph/9912492] [INSPIRE].

[24] S.F. King, *Constructing the large mixing angle MNS matrix in seesaw models with right-handed neutrino dominance*, *JHEP* **09** (2002) 011 [hep-ph/0204360] [INSPIRE].

[25] E. Ma and G. Rajasekaran, *Softly broken A_4 symmetry for nearly degenerate neutrino masses*, *Phys. Rev.* **D 64** (2001) 113012 [hep-ph/0106291] [INSPIRE].

[26] S.F. King and C. Luhn, *On the origin of neutrino flavour symmetry*, *JHEP* **10** (2009) 093 [arXiv:0908.1897] [INSPIRE].

[27] S.F. King, T. Neder and A.J. Stuart, *Lepton mixing predictions from $\Delta(6n^2)$ family Symmetry*, *Phys. Lett.* **B 726** (2013) 312 [arXiv:1305.3200] [INSPIRE].

[28] H. Ishimori and S.F. King, *A model of quarks with Delta $(6N^2)$ family symmetry*, arXiv:1403.4395 [INSPIRE].

[29] M. Holthausen and K.S. Lim, *Quark and Leptonic Mixing Patterns from the Breakdown of a Common Discrete Flavor Symmetry*, *Phys. Rev.* **D 88** (2013) 033018 [arXiv:1306.4356] [INSPIRE].

[30] S.F. King, *Predicting neutrino parameters from SO(3) family symmetry and quark-lepton unification*, *JHEP* **08** (2005) 105 [hep-ph/0506297] [INSPIRE].

[31] S. Antusch, S.F. King, C. Luhn and M. Spinrath, *Trimaximal mixing with predicted θ_{13} from a new type of constrained sequential dominance*, *Nucl. Phys.* **B 856** (2012) 328 [arXiv:1108.4278] [INSPIRE].

[32] S. Antusch, S.F. King and M. Spinrath, *Spontaneous CP-violation in $A_4 \times$ SU(5) with Constrained Sequential Dominance 2*, *Phys. Rev.* **D 87** (2013) 096018 [arXiv:1301.6764] [INSPIRE].

[33] S.F. King, *Minimal predictive see-saw model with normal neutrino mass hierarchy*, *JHEP* **07** (2013) 137 [arXiv:1304.6264] [INSPIRE].

[34] S.F. King, *Minimal see-saw model predicting best fit lepton mixing angles*, *Phys. Lett.* **B 724** (2013) 92 [arXiv:1305.4846] [INSPIRE].

[35] S.F. King, *A model of quark and lepton mixing*, *JHEP* **01** (2014) 119 [arXiv:1311.3295] [INSPIRE].

[36] J.C. Pati and A. Salam, *Lepton Number as the Fourth Color*, *Phys. Rev.* **D 10** (1974) 275 [*Erratum ibid.* **D 11** (1975) 703-703] [INSPIRE].

JHEP08(2014)130

[37] S.F. King and M. Malinsky, *A_4 family symmetry and quark-lepton unification*, *Phys. Lett.* **B 645** (2007) 351 [hep-ph/0610250] [INSPIRE].

[38] A. Karozas, S.F. King, G.K. Leontaris and A. Meadowcroft, *Discrete Family Symmetry from F-theory GUTs*, arXiv:1406.6290 [INSPIRE].

[39] I. Antoniadis and G.K. Leontaris, *Neutrino mass textures from F-theory*, *Eur. Phys. J.* **C 73** (2013) 2670 [arXiv:1308.1581] [INSPIRE].

[40] I. Antoniadis, G.K. Leontaris and J. Rizos, *A three generation* $\mathrm{SU}(4) \times O(4)$ *string model*, *Phys. Lett.* **B 245** (1990) 161 [INSPIRE].

[41] S.F. King and Q. Shafi, *Minimal supersymmetric* $\mathrm{SU}(4) \times \mathrm{SU}(2)_L \times \mathrm{SU}(2)_R$, *Phys. Lett.* **B 422** (1998) 135 [hep-ph/9711288] [INSPIRE].

[42] S. Antusch, S.F. King and M. Spinrath, *Spontaneous CP-violation in* $A_4 \times \mathrm{SU}(5)$ *with Constrained Sequential Dominance 2*, *Phys. Rev.* **D 87** (2013) 096018 [arXiv:1301.6764] [INSPIRE].

[43] S. Antusch, S.F. King, C. Luhn and M. Spinrath, *Right Unitarity Triangles and Tri-Bimaximal Mixing from Discrete Symmetries and Unification*, *Nucl. Phys.* **B 850** (2011) 477 [arXiv:1103.5930] [INSPIRE].

[44] M. Holthausen, M. Lindner and M.A. Schmidt, *CP and Discrete Flavour Symmetries*, *JHEP* **04** (2013) 122 [arXiv:1211.6953] [INSPIRE].

[45] G.-J. Ding, S.F. King and A.J. Stuart, *Generalised CP and A_4 Family Symmetry*, *JHEP* **12** (2013) 006 [arXiv:1307.4212] [INSPIRE].

[46] I. de Medeiros Varzielas and D. Emmanuel-Costa, *Geometrical CP-violation*, *Phys. Rev.* **D 84** (2011) 117901 [arXiv:1106.5477] [INSPIRE].

[47] I. Medeiros Varzielas and D. Pidt, *Geometrical CP-violation with a complete fermion sector*, *JHEP* **11** (2013) 206 [arXiv:1307.6545] [INSPIRE].

[48] G.-J. Ding, S.F. King, C. Luhn and A.J. Stuart, *Spontaneous CP-violation from vacuum alignment in S_4 models of leptons*, *JHEP* **05** (2013) 084 [arXiv:1303.6180] [INSPIRE].

[49] F. Feruglio, C. Hagedorn and R. Ziegler, *A realistic pattern of lepton mixing and masses from S_4 and CP*, *Eur. Phys. J.* **C 74** (2014) 2753 [arXiv:1303.7178] [INSPIRE].

[50] F. Feruglio, C. Hagedorn and R. Ziegler, *Lepton Mixing Parameters from Discrete and CP Symmetries*, *JHEP* **07** (2013) 027 [arXiv:1211.5560] [INSPIRE].

[51] S.F. King and T. Neder, *Lepton Mixing Predictions including Majorana Phases from $\Delta(6n^2)$ Flavour Symmetry and Generalised CP*, arXiv:1403.1758 [INSPIRE].

[52] C.H. Albright, *A nonminimal* $\mathrm{SO}(10) \times \mathrm{U}(1)_{\mathrm{F}}$ *SUSY GUT model obtained from a bottom up approach*, *Eur. Phys. J.* **C 1** (1998) 657 [hep-ph/9608372] [INSPIRE].

[53] H. Georgi and C. Jarlskog, *A New Lepton-Quark Mass Relation in a Unified Theory*, *Phys. Lett.* **B 86** (1979) 297 [INSPIRE].

[54] S. Antusch, S.F. King and M. Spinrath, *GUT predictions for quark-lepton Yukawa coupling ratios with messenger masses from non-singlets*, *Phys. Rev.* **D 89** (2014) 055027 [arXiv:1311.0877] [INSPIRE].

[55] D. Aristizabal Sierra, M. Tortola, J.W.F. Valle and A. Vicente, *Leptogenesis with a dynamical seesaw scale*, *JCAP* **07** (2014) 052 [arXiv:1405.4706] [INSPIRE].

JHEP08(2014)130

[56] Particle Data Group collaboration, J. Beringer et al., *Review of Particle Physics (RPP)*, *Phys. Rev.* **D 86** (2012) 010001 [INSPIRE].

[57] S. Antusch, J. Kersten, M. Lindner, M. Ratz and M.A. Schmidt, *Running neutrino mass parameters in see-saw scenarios*, *JHEP* **03** (2005) 024 [hep-ph/0501272] [INSPIRE].

[58] S.F. King and N.N. Singh, *Renormalization group analysis of single right-handed neutrino dominance*, *Nucl. Phys.* **B 591** (2000) 3 [hep-ph/0006229] [INSPIRE].

[59] S. Boudjemaa and S.F. King, *Deviations from Tri-bimaximal Mixing: Charged Lepton Corrections and Renormalization Group Running*, *Phys. Rev.* **D 79** (2009) 033001 [arXiv:0808.2782] [INSPIRE].

[60] S. Antusch, S.F. King and M. Malinsky, *Third Family Corrections to Tri-bimaximal Lepton Mixing and a New Sum Rule*, *Phys. Lett.* **B 671** (2009) 263 [arXiv:0711.4727] [INSPIRE].

[61] S. Antusch, S.F. King and M. Malinsky, *Third Family Corrections to Quark and Lepton Mixing in SUSY Models with non-Abelian Family Symmetry*, *JHEP* **05** (2008) 066 [arXiv:0712.3759] [INSPIRE].

[62] S. Antusch, S.F. King and M. Malinsky, *Perturbative Estimates of Lepton Mixing Angles in Unified Models*, *Nucl. Phys.* **B 820** (2009) 32 [arXiv:0810.3863] [INSPIRE].

[63] S.F. King, *Parametrizing the lepton mixing matrix in terms of deviations from tri-bimaximal mixing*, *Phys. Lett.* **B 659** (2008) 244 [arXiv:0710.0530] [INSPIRE].

[64] W. Winter, *Neutrino mass hierarchy determination with IceCube-PINGU*, *Phys. Rev.* **D 88** (2013) 013013 [arXiv:1305.5539] [INSPIRE].

[65] S. Choubey and A. Ghosh, *Determining the Octant of θ_{23} with PINGU, T2K, NOνA and Reactor Data*, *JHEP* **11** (2013) 166 [arXiv:1309.5760] [INSPIRE].

[66] M. Blennow, P. Coloma, P. Huber and T. Schwetz, *Quantifying the sensitivity of oscillation experiments to the neutrino mass ordering*, *JHEP* **03** (2014) 028 [arXiv:1311.1822] [INSPIRE].

[67] S.-F. Ge, K. Hagiwara and C. Rott, *A Novel Approach to Study Atmospheric Neutrino Oscillation*, *JHEP* **06** (2014) 150 [arXiv:1309.3176] [INSPIRE].

[68] S.-F. Ge and K. Hagiwara, *Physics Reach of Atmospheric Neutrino Measurements at PINGU*, arXiv:1312.0457 [INSPIRE].

[69] L. Zhan, *Daya Bay II and Future Reactor Experiments*, *Nucl. Phys. Proc. Suppl.* **237-238** (2013) 114 [INSPIRE].

[70] S.-F. Ge, K. Hagiwara, N. Okamura and Y. Takaesu, *Determination of mass hierarchy with medium baseline reactor neutrino experiments*, *JHEP* **05** (2013) 131 [arXiv:1210.8141] [INSPIRE].

[71] P. Ballett, S.F. King, C. Luhn, S. Pascoli and M.A. Schmidt, *Precision measurements of θ_{12} for testing models of discrete leptonic flavour symmetries*, arXiv:1406.0308 [INSPIRE].

[72] P. Ballett, S.F. King, C. Luhn, S. Pascoli and M.A. Schmidt, *Testing atmospheric mixing sum rules at precision neutrino facilities*, *Phys. Rev.* **D 89** (2014) 016016 [arXiv:1308.4314] [INSPIRE].

JHEP08(2014)130